IMPLEMENTATION OF NULL STEERING ALGORITHMS IN A COMPACT ANALOG ARRAY

by

Hugo Orlando Condori Quispe

A thesis submitted in partial fulfillment
of the requirements for the degree

of

Master of Science

in

Electrical Engineering

MONTANA STATE UNIVERSITY
Bozeman, Montana

April, 2014

© COPYRIGHT

by

Hugo Orlando Condori Quispe

2014

All Rights Reserved

ACKNOWLEDGEMENTS

This stage of my life as a graduate student at Montana State University has been one of the most memorable in my life. I would like to thank many people that have contributed in many ways in this journey.

I want to give thanks to my adviser Prof. Richard Wolff. I am grateful for all his help and for giving me the freedom to pursue my ideas in research and providing unconditional support during my stage at Montana State University. My gratitude goes to my thesis committee: Prof. Yikun Huang and Prof. Ross Snider. Prof. Huang has been constant source of support during the development of this work. Uncountable hours of technical discussions were given to discuss the status of the project and future directions.

I would like to gratefully acknowledge the support of the Fulbright Scholarship which made this work possible.

Every result described in this thesis was accomplished with the help and support of fellow lab mates. I am especially grateful to a great friend Aditya Angampally. I have had the great pleasure to work with him on this project, through all the ups and downs of the countless hours that we spent together in the communications lab trying to make our experiments work (some of them did actually). I would like to acknowledge Raymond Weber for his assistance and contributions on this project.

TABLE OF CONTENTS

1. INTRODUCTION 1

Motivation 1
Null Steering 1
Project Definition 4
Overview 5

2. SYSTEM OVERVIEW 6

Antenna Array 6
Analog Beamformer Board 7

3. NULL STEERING ALGORITHMS 9

Data Model 9
Null Steering Algorithms 11
Open-loop Null Steering 12
Optimal Null Steering Algorithm 12
Waveform Modification 13
Closed-loop Null Steering 14

4. SIMULATION STUDY 17

Null Steering Performance Analysis 17
Null Patterns 17
Cumulative Distribution Function Analysis 18
Case I: Null Inside the Main Beam 19
Case II: Null Outside the Main Beam 24
Phase and Magnitude Errors 27
Phase Error Analysis 27
Magnitude Analysis 29
Quantization Error and Phase Perturbation 33
Multiple Nulls 38

5. LAB TESTS 40

Lab Setup 40
Lab Test Results 44

TABLE OF CONTENTS – CONTINUED

6. CONCLUSION AND FUTURE WORK 47

Conclusions 47
Future Work 48

REFERENCES CITED 48

LIST OF TABLES

Table Page

4.1 Uniform Circular Antenna Array Characteristics 18
4.2 Simulation Null Steering Results 18
4.3 CDF Values Summary for Case I 23
4.4 CDF Values Summary for Case II 26
4.5 Multi-null Steering Results for the Optimal Null Steering Algorithm 38
5.1 Experimental Null Steering Results 45

LIST OF FIGURES

Figure Page

1.1 Null steering to the interference signal 3
2.1 Circular antenna array 6
2.2 Beamformer board with the UCA 7
2.3 Beamformer board block diagram 8
3.1 Diagram of the antenna array 10
3.2 System output interference to signal ratio $E(OISR)$ 13
3.3 Illustration of the waveform modification algorithm 14
3.4 Diagram of closed-loop adaptive null steering algorithm 15
4.1 Beam pattern for the optimal null steering algorithm 19
4.2 Beam pattern for the waveform modification null steering algorithm 20
4.3 Beam pattern for the adaptive null steering algorithm 20
4.4 Beam pattern for case I 21
4.5 CDF for case I using the optimal null steering algorithm 22
4.6 CDF for case I using the waveform modification algorithm 22
4.7 CDF for case I using the LMS algorithm 23
4.8 Beam pattern for case II 24
4.9 CDF for case II using the optimal null steering algorithm 25
4.10 CDF for case II using the waveform modification algorithm 25
4.11 CDF for case II using LMS null steering algorithm 26
4.12 Effect of the phase errors on the power pattern 28
4.13 Effect of the phase error for the optimal null steering algorithm 29
4.14 Effect of the phase error for the waveform modification algorithm 30
4.15 Effect of the phase error for the LMS null steering algorithm 30
4.16 Effect of the magnitude error for the optimal null steering algorithm 31

LIST OF FIGURES – CONTINUED

Figure Page

4.17 Effect of the magnitude error for the waveform modification algorithm ... 31
4.18 Effect of the magnitude error for the LMS null steering algorithm 32
4.19 Effect of 10% magnitude error on the power pattern 33
4.20 Effect of 20% magnitude error on the power pattern 34
4.21 Effect of the magnitude error for the optimal null steering algorithm 34
4.22 Effect of the magnitude error for the waveform modification algorithm ... 35
4.23 Effect of the magnitude error for the LMS null steering algorithm 35
4.24 Beam pattern without phase perturbation 36
4.25 Beam pattern with phase perturbation 37
4.26 Beam pattern for the optimal multi-null steering algorithm 39
5.1 Block diagram of the lab test set up for receiving null steering 41
5.2 Anechoic chamber 42
5.3 Instruments 42
5.4 Beam pattern for the optimal null steering algorithm 44
5.5 Beam pattern for the waveform modification null steering algorithm 45
5.6 Beam pattern for the LMS adaptive null steering algorithm 46

ABSTRACT

In this thesis, the implementation of null steering algorithms in a compact analog array is demonstrated and validated. The performance of the null steering algorithms is validated through extensive simulation and hardware implementation. The results of the techniques of null steering, including controlling the complex weights, usually have to rely on simulations to study system performances, design trade-offs, and system optimization, which by itself can be quite complex and a time-consuming task. Even after extensive simulations, it is not easy to get insights as to what parameters determine system performance in different system parameters, and the interactions on system parameters. Therefore, experimentation and deployment on a real system is required. Few studies have proposed null steering algorithms studies using real implementations. With this motivation, this work presents comprehensive performance comparison of some of the available null steering techniques using an analog array. The contributions of this thesis are: optimize the performance of null steering algorithms taking into account realistic considerations in the simulations and demonstrating the benefits through extensive simulations; and verify the performance of the null steering system through experimental implementation using a simple, compact, lightweight, low cost, high gain, high throughput analog antenna array.

1

INTRODUCTION

Motivation

One of the major problems of security in military radars and wireless communications is jamming. Due to their open and ubiquitous nature, wireless communication systems are extremely vulnerable to attack. Jamming, defined as the use of active signals to prevent data distribution, has emerged as an attractive attack method [1]. In this attack, the adversary tries to prevent or interfere with the reception of signals at the nodes in the network. Most current data communication standards, such as IEEE802.16 and Bluetooth [2], are not designed to resist malicious interference; a small number of jammers with limited energy resources can disrupt operation of an entire network. In addition, jamming is a common method of attack in military networks where transmissions are often performed in the presence of an adversary whose goal is to disrupt the communication to a maximum degree [3].

Different security mechanisms and countermeasures against jamming for defending the attacks have been proposed in literature. A survey describing the anti-jamming countermeasures can be found in [4].

Null Steering

Null steering is one of the efficient methods to counter jamming attacks. The techniques of placing nulls in the antenna array pattern to suppress jamming signals and maximize its gain toward the direction of the desired signal has received considerable attention in the past and it is still of great interest [5]. Implementation of a null steering algorithm in an antenna array implies that the antenna array can be

used to steer nulls in the direction of known interference signals while maintaining the main beam toward a desired direction [6]. This improves the performance of the antenna system enhancing the Signal to Interference Ratio (SIR) by suppressing the interference signal [5]. However, null steering methods have seen limited use due to the cost and size of the array system. If null steering is available in the analog Radio Frequency (RF) stage of antenna arrays, it can provide drastic improvement in both Direct Current (DC) power dissipation and fabrication costs, an improvement that is proportional to the number of array elements [6].

Null steering algorithms rely on controlling the weights of the antenna array. Since the parameters of the null steering weights follow a complex form, null steering can be controlled by changing only the amplitude, only the phase of the weights or both.

Null steering methods that change only the phase of the null steering weights have been extensively considered in the literature [7, 8, 9, 10] . In [7], the null steering method proposed is based on the adaptive Sequential Quadratic Programming (SQP) algorithm that transforms the nonlinear minimization problem to a sequence of quadratic sub-problems. This method works efficiently when multiple users are targeted while simultaneously nulling the interference. Another technique was proposed by Zhu et al. [8], where the phases of the null steering weights are calculated using genetic algorithms. The method modeled and targeted linear arrays. By using this technique, it was possible to steer the null toward the interference angular location and simultaneously minimize the maximum sidelobe level. Another method for phase-only null steering is proposed by Ananasso [9]. In this method the performance of the null-steering system, using digital phase-only weights, is analyzed numerically by a computer simulation. Another genetic algorithm approach has been proposed by Haupt and Haupt [10]. The authors demonstrate that it is possible to control the phases only of the null steering weights following a genetic algorithm, and place

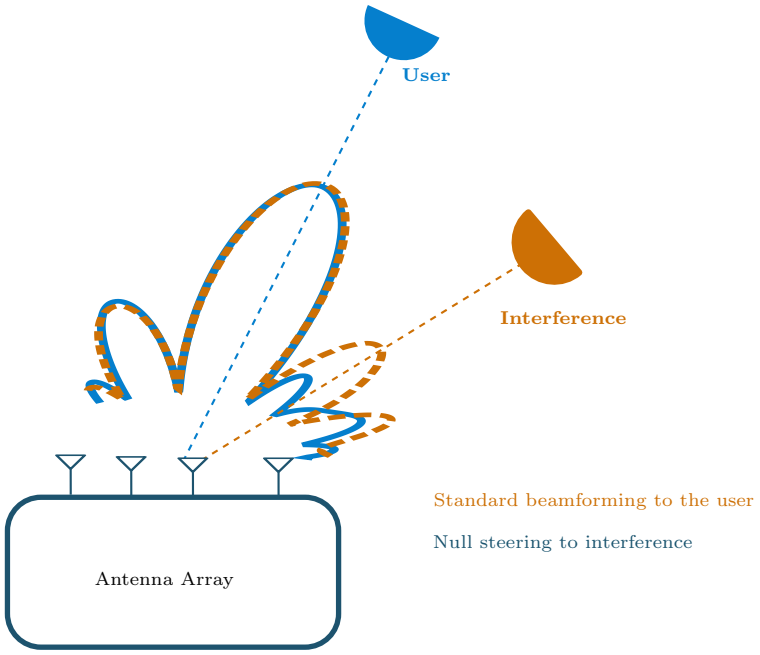


Figure 1.1: Null steering to the interference signal

multiple deep nulls in the directions of the interferences. This genetic algorithm takes into account the quantization errors of the weights introduced when the algorithms are implemented in hardware. The authors demonstrate that it is possible to achieve deep nulls at the direction of the interferences while having a low side lobe level. One disadvantage of this method is that it relies on the utilization of a high number of elements to easily converge to the solution of the null steering weights.

Null steering methods that rely on the changes of the magnitude-only have also been studied and different approaches can be found in the literature [11, 12]. The author in [11] proposes a method of null steering controlling only the magnitude of the weights; therefore excluding the phase shifters when performing null steering. The author demonstrates the functionality of the algorithm, using an 8 element linear array, by forcing the nulls in such a way that the zeros of the power pattern of the antenna array occurs in conjugate pairs. Genetic algorithms have been proposed to

calculate the null steering weights by controlling only the magnitude. Yallaparagada et al. [12] reported a genetic algorithm for null steering in a circular antenna array. One of the major drawbacks in this algorithm is the number of convergence cycles necessary to arrive at a final solution.

Another approach for calculating the null steering weights relies on changes of the phase as well as the magnitude [5, 13, 14, 15, 16]. In this thesis, a comprehensive performance comparison of some of the available null steering techniques was performed. The parameters taken into account for comparison were null depth, side lobe level, and SIR.

Project Definition

The goal of this thesis is to provide a realistic evaluation of the performance of null steering techniques targeting the implementation in a simple, compact, lightweight, low cost, high gain, high throughput, analog antenna array with efficient null steering performance. The performance of the algorithms is validated through extensive simulations and hardware implementation. This thesis consolidates the work presented in [17, 18, 19, 20, 5].

The results of the techniques of null steering, including controlling the complex weights, usually have to rely on simulations to study system performances, design trade-offs, and system optimization, which by itself can be quite complex and a time-consuming task. Even after extensive simulations, it is not easy to get insights as to what parameters determine system performance in different system parameters, and the interactions on system parameters. Therefore, experimentation and deployment on a real system is required. Few studies have proposed null steering algorithms studies using real implementations. With this motivation, this work presents com-

prehensive performance comparison of some of the available null steering techniques using an analog array.

The contributions of this thesis are two fold:

- optimizing the performance of null steering algorithms taking into account realistic considerations in the simulations and demonstrating the benefits through extensive simulations;
- verifying the performance of the null steering system through extensive simulations and experimental implementation using a simple, compact, lightweight, low cost, high gain, high throughput analog antenna array.

Overview

The thesis is divided into six chapters. Chapter 2 describes the hardware system utilized to prove and evaluate the performance of the null steering algorithms. Chapter 3 describes the rationale behind the null steering algorithms studied and implemented. Chapter 4 contains the results of the simulation of the null steering algorithms. Chapter 5 presents the experimental results obtained after implementing the null steering algorithms in an analog antenna array. The conclusions and discussion of future work are presented in the last chapter.

6

SYSTEM OVERVIEW

Antenna Array

The uniform circular antenna array (UCA) developed at Montana State University (MSU) is an 8 element UCA, composed of two functional blocks: the thin-wire monopole apertures and the ground plane with ground skirt as shown in Figure 2.1. The ground plane and skirt provide a virtual infinite ground plane and mechanical rigidity [21, 22]. The array has an operating center frequency of 5.8 GHz and spatially covers 360° in the azimuth plane. The array electrical size is $\beta\rho = 3.05$, where β is the wave number, ρ is the array radius, 2.54 cm. The inter-element spacing is 0.375λ and the antenna element length is 0.23λ. The array gain is $12 - 15$ dBi depending on the algorithm used in weighting the beamformer channels. The operating bandwidth of 200 MHz centered about 5.8 GHz has relatively flat gain [23, 24].

The beam patterns of the array were measured in the anechoic chamber at the Communications Lab at MSU. The chamber size is $41.74'' \times 79.5'' \times 51.5''$ ($W \times L \times H$). The frequency range of the chamber is 2GHz−30GHz and the microwave absorber thickness is: 5 inches (−42dB) and 8 inches (−52dB). A 5.8 GHz resonant horn antenna (WR159 $f = 4.9 - 7.05$ GHz) is located at one end of the chamber [25]. The

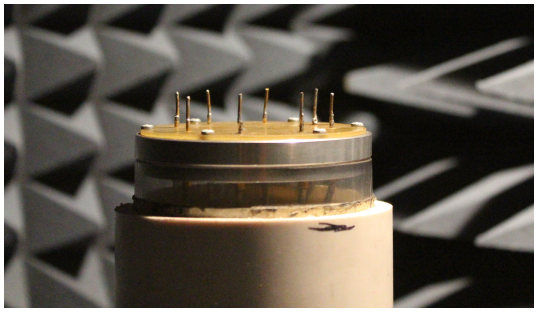


Figure 2.1: Circular antenna array

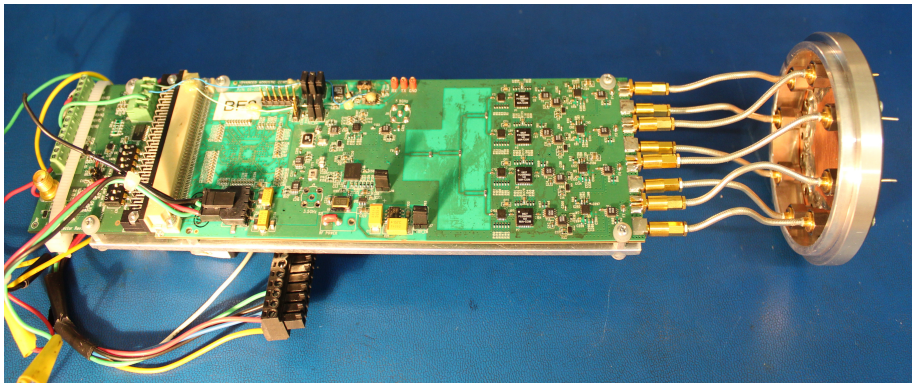


Figure 2.2: Beamformer board with the UCA

other end of the chamber has a rotating pedestal with a stepper motor attached. The antenna array is mounted on the rotating pedestal, controlled by the step motor with a personal computer (PC) through a Data AcQuisition card (DAQ), which allows it to collect a full 360° power spectrum [17]. The pedestal is built to hold the complete antenna array system.

Analog Beamformer Board

The purpose of the RF beamformer board is to apply the PC generated beamforming weights to the RF signal coming from the array so that the directional beam is formed.

A photo of the beamformer board is shown in Figure 2.2 and a block diagram can be seen in Figure 2.3. The beamformer board is an 8 channel digitally controlled analog beamforming system that controls phase and amplitude of each channel to form a beam in the desired direction. The beamforming system consists of five functional blocks: controller, analog beamforming circuitry, radio interface, power detection, and power regulation [25]. The controlling unit provides digital control via

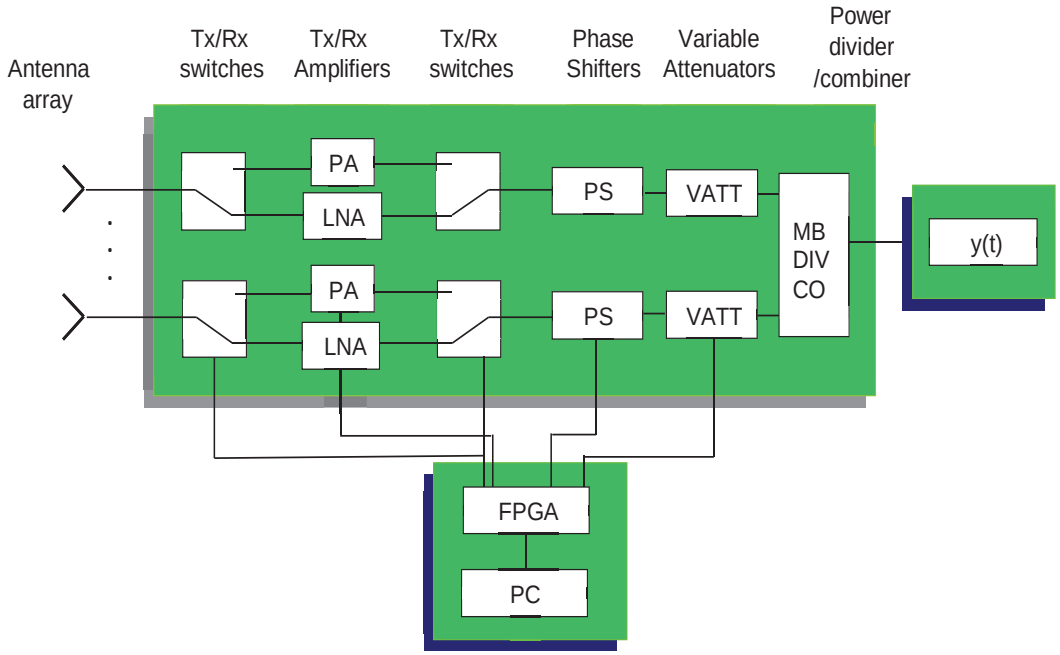


Figure 2.3: Beamformer board block diagram

an Field-Programmable Gate Array (FPGA) (Xilinx Spartan-3). The FPGA delivers 96 parallel control lines to eight 6−bit phase shifters (MAPCGM0002) and eight 6−bit attenuators (HMC425LP3) [18, 26]. The 6−bit phase shifters can produce phase changes between $-180°$ and $+180°$ in $5.6°$ increments. The attenuation range is 0 to -31.5 dB in increments of 0.5 dB [18].

The beamformer board contains power amplifiers (SZA−5033) and low noise amplifiers (HMC320MS8G) as well as switches that toggle the channels between transmission and receiving modes. Another component of this board is a Xilinx CoolRunnerII Complex Programmable Logic Device (CPLD). The CPLD receives the control information from the PC and uses it to directly control the phase shifters and attenuators. The device was programmed to implement a shift register which acquires serial data from the PC and latches it out to the individual channels in parallel [27, 28, 29].

NULL STEERING ALGORITHMS

In this chapter, the data model and the null steering algorithms implemented in an analog antenna array, are described.

Data Model

An m element array with an arbitrary geometry is considered. The array can receive signals from K different sources located in different angular locations. The signal arriving to the antenna array, $\mathbf{x}(t)$ can be expressed as:

$$\mathbf{x}(t) = \sum_{k=1}^{K} \boldsymbol{a}\left(\varphi_k\right) s_k(t) + \boldsymbol{n}(t) \tag{3.1}$$

where

$s_k(t)$ is the kth impinging signal.

$\boldsymbol{a}(\varphi_k)$ is the spatial signature of the signal s_k from φ_k.

φ_k is the direction of arrival of the kth signal.

$\boldsymbol{n}(t)$ is the noise at the receiver site.

K is the number of signals received by the smart antenna array.

In this thesis, the simulations study and the implementation of the algorithms consider the characteristics of a UCA. The circular antenna array configuration was chosen because of access of pre-existing UCA hardware developed at MSU, see [30, 25].

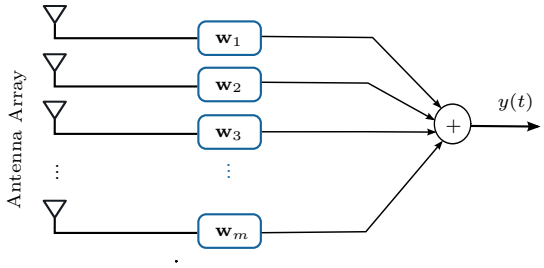


Figure 3.1: Diagram of the antenna array

The spatial signature of the uniform circular antenna array at relevant angles, θ and φ, is defined as the following [31]:

$$\boldsymbol{a}\left(\varphi,\theta\right)=\left[1,e^{j\beta\rho\sin(\theta)\cos\left(\varphi-\frac{2\pi}{m}\right)},e^{j\beta\rho\sin(\theta)\cos\left(\varphi-\frac{2\cdot2\pi}{m}\right)},...,e^{j\beta\rho\sin(\theta)\cos\left(\varphi-\frac{(m-1)\cdot2\pi}{m}\right)}\right] \quad (3.2)$$

where

φ is the azimuthal angle.

θ is the elevation angle.

β is the wavenumber defined as: $\beta=\frac{2\pi}{\lambda}$.

$\beta\rho$ is the electrical size of the array.

As shown in Figure 3.1, the m channels of the antenna data are scaled and shifted by the weight values, and the linear combination is the output of the beamformer, $y(t)$, defined as:

$$\begin{aligned} y(t) &= \boldsymbol{w}^H\cdot\mathbf{x}\left(t\right) \\ &= \boldsymbol{w}^H\cdot\sum_{k=1}^{K}\boldsymbol{a}\left(\varphi_k\right)s_k(t)+\boldsymbol{w}^H\cdot\boldsymbol{n}(t) \end{aligned} \quad (3.3)$$

where

$\boldsymbol{w}$ is the null-steering weight vector for the antenna array.

H is the complex conjugate transpose.

Assuming that the direction of arrival (DOA) of one user signal is φ_d; and the DOA of one interference signal is φ_{int}; equation 3.3 takes the form:

$$y(t) = \boldsymbol{w}^H \cdot \boldsymbol{a}\left(\varphi_d\right) s_d(t) + \boldsymbol{w}^H \cdot \boldsymbol{a}\left(\varphi_{int}\right) s_{int}(t) + \boldsymbol{w}^H \cdot \boldsymbol{n}(t) \tag{3.4}$$

The Signal to Interference Ratio (SIR) allows evaluation of the performance of the algorithms in the presence of K_n interference signals; in this thesis, the SIR is calculated as shown in equation 3.5 [32] :

$$SIR = \frac{S}{I} = \frac{S}{\sum_{k=1}^{K_n} I_k} \tag{3.5}$$

Null Steering Algorithms

Interference cancellation can be achieved by suppressing the power density at the angle of the interference signal. This is achieved by properly scaling and phase shifting the UCA element currents, such that the power received at the interference angular direction is minimized. The constraints for the null steering weights are:

- Minimize $\boldsymbol{w}^H \cdot \boldsymbol{a}\left(\varphi_{int}\right)$
- Maximize $\boldsymbol{w}^H \cdot \boldsymbol{a}\left(\varphi_d\right)$
- Mantain $\boldsymbol{w}^H \cdot \boldsymbol{w}$ constant

The algorithms studied in this thesis can be categorized into two groups. The first group corresponds to open-loop null steering methods; these algorithms rely on

the previous estimation of the DOA of the interference and the user signal sources. The second group corresponds to closed-loop adaptive null steering methods where the nulls are formed adaptively and no previous knowledge of the DOAs is required in advance.

Open-loop Null Steering

Open-loop null steering algorithms involve a two-step solution. The first step consists of estimating the directions of arrival of all wavefronts impinging on an antenna array. The second step consists of forming nulls in the estimated directions of the interference signal, while maximizing the received signals [13].

Two different open-loop null steering algorithms were analyzed and implemented in the UCA and are described below.

Optimal Null Steering Algorithm: This algorithm was first proposed by Friedlander and Porat [13]. The null steering weights were defined using matrix subspace algebra to separate the signal space from the interference space and uses a vector null space to achieve the maximum signal minimum noise criteria.

The null steering weights are calculated as follows:

$$\boldsymbol{w} = \left[\mathbf{I} - \boldsymbol{a}(\varphi_{int}) \left(\boldsymbol{a}(\varphi_{int})^H \cdot \boldsymbol{a}(\varphi_{int})\right)^{-1} \cdot \boldsymbol{a}(\varphi_{int})^H\right] \boldsymbol{a}(\varphi_d) \tag{3.6}$$

where $\mathbf{I}$ is the identity matrix.

An analytical study of the expectation of the system output interference to signal ratio E(OSIR) versus the angular space between DOA of the interference signal φ_{int} and the desired signal φ_d was proposed and studied in [13, 33]. The optimal weight defined in Equation 3.6 was used. In Figure 3.2, the DOA of the desired signal is

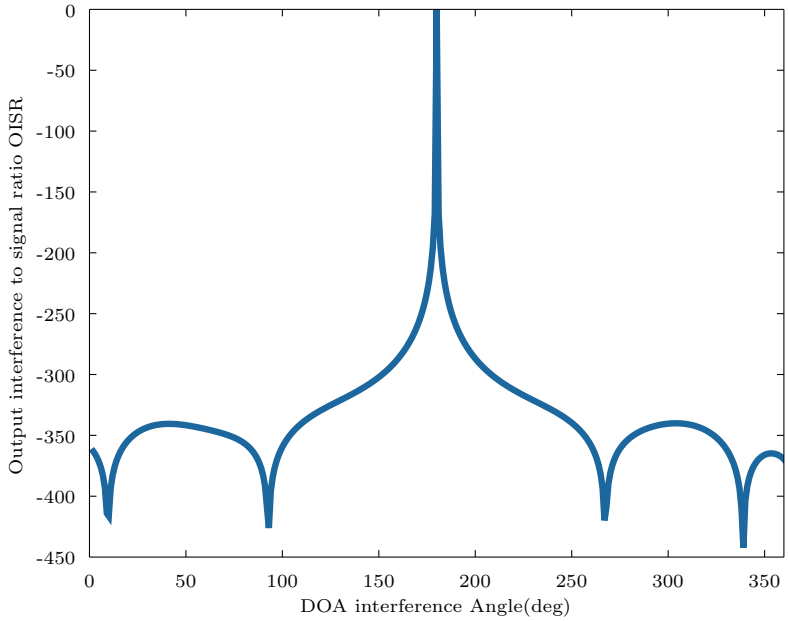


Figure 3.2: System output interference to signal ratio $E(OISR)$

$\varphi_d = 180°$ and the DOA of the interference signal takes values in the range from $[0° - 360°]$. Note that in Figure 3.2 we have $OISR = \frac{P_{int}}{P_d} = 0$ dB at $\varphi_d = \varphi_{int} = 180°$ as expected.

Waveform Modification: The second method is based on waveform modification proposed by Y. Huang and M. Panique [33].

This method makes use of element current phase and magnitude perturbation. The algorithm starts with independent beamforming weights for both the desired signal and interference as shown in Figure 3.3. The weights for null steering are calculated by taking the linear difference of the two sets of weights.

$$\boldsymbol{w} = \boldsymbol{a}(\varphi_d) - c \cdot \boldsymbol{a}(\varphi_{int}) \tag{3.7}$$

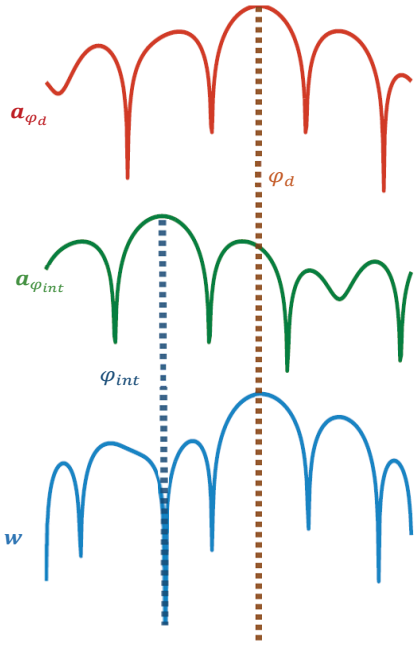


Figure 3.3: Illustration of the waveform modification algorithm

The constant c is defined as the linear difference in power between the beams formed by $\boldsymbol{a}(\varphi_d)$, the angular location of the user signal, and $\boldsymbol{a}(\varphi_{int})$ at the angular location of the interference, φ_{int}.

Closed-loop Null Steering

Closed-loop adaptive null steering algorithms are more robust than open-loop algorithms since they can adjust to uncertainties in the phase-gain characteristics of the array elements and do not require array calibration. Moreover, these algorithms do not require the knowledge of the DOAs of the sources in advance. The adaptive null steering methods utilize sophisticated signal processing algorithms to continuously distinguish between the desired signal and interferences without knowing the DOAs of the desired signal and interference in advance. It can form an unlimited number of beam patterns to optimally improve signal strength and suppress interference signals.

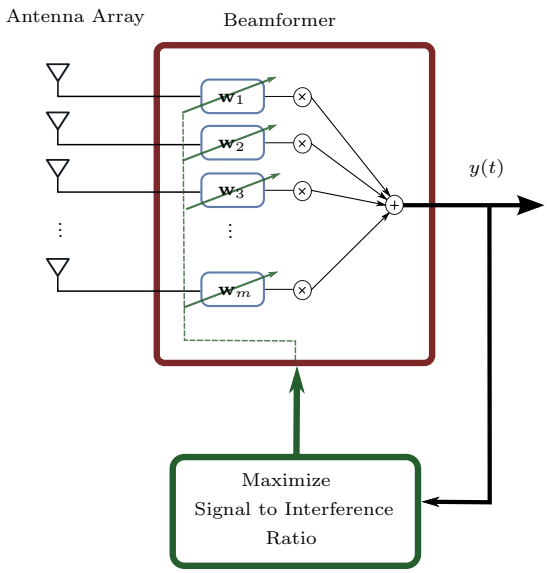


Figure 3.4: Diagram of closed-loop adaptive null steering algorithm

These algorithms are fairly simple to implement; they rely on an iterative process, the final set of weights may not be a truly optimal setting [6]. Although mathematically elegant and efficient, the solution given by this method might not be the optimal, giving as a solution the local minima around the vicinity of the starting point [34].

The adaptive weight $\boldsymbol{w}$ can be obtained using any suitable adaptive algorithms as shown in Figure 3.4. Here, we use Least Mean Square (LMS) algorithm for proof of concept, assuming the reference signal $s(t)$ is known

$$\min_{\epsilon} \left| \boldsymbol{w}_{adaptive}^{H} \cdot \mathbf{x}(t) - s(t) \right|^2 \tag{3.8}$$

The output of the beamformer is

$$y(t) = \boldsymbol{w}_{adaptive}^{H} \cdot \mathbf{x}(t) \tag{3.9}$$

The advantages of adaptive null steering algorithms are its superior flexibility and efficient adjustment to uncertainties in the phase and amplitude oscillations of the null steering weights.

SIMULATION STUDY

In this chapter, the performance of the algorithms is validated. The simulations were constructed to demonstrate the performance of the algorithms described in chapter 3. The UCA consists of 8 elements as described in Chapter 2. A summary table with its dimensions is shown in table 4.1.

Simulation data collection and statistical processing were carried out using a combination of scripts and functions in MATLAB. Custom functions were written to model the antenna array.

Null Steering Performance Analysis

Some simulation results are discussed to verify the functionality of the algorithms presented in Chapter 3. The main parameters that were used to evaluate the performance of the null steering algorithms were the SIR and the pointing angle. The SIR is obtained by taking the ratio between the energy at the angular location of the user and the energy at the angular location of the interference as defined in equation 3.5.

For the results presented, the interference signal DOA is assumed to be at 300 °; the desired signal DOA is assumed to be at 180 °. The signal to noise ratio is assumed to be 20 dB The power plots were normalized, unless noted otherwise.

Null Patterns

Figure 4.1 shows the null steering beam pattern using the optimal null steering algorithm. Note that the main beam is pointing to the user signal angular location; there is a null at the angular location of the interference signal. The SIR in this case is 64.43 dB. Similar analysis was performed for the waveform modification algorithm,

Table 4.1: Uniform Circular Antenna Array Characteristics

Number of elements	8
Operating frequency (GHz)	5.8
Bandwidth (MHz)	200
Array radious ρ(cm)	2.54
Array electrical size $\beta\rho$	3.05
Inter-element Spacing	0.375λ
Element length	0.23λ

Table 4.2: Simulation Null Steering Results

Method	φ_d [°]	φ_{int} [°]	SIR[dB]
Optimal null steering	180	300	64.43
Waveform modification	180	300	59.33
LMS null steering	180	300	59.33

Figure 4.2. A maximum was observed at the angular location of the user signal and a deep null at the location of the interference. The SIR obtained is 59 dB.

The results for the LMS algorithm is shown in Figure 4.3. There is a deep null at the angular location of the interference signal and the SIR is 59 dB.

The summary of the results obtained after setting up this scenario for the three algorithms described in Chapter 3 are shown in Table 4.2.

Cumulative Distribution Function Analysis

A key point of the analysis of these algorithms is the resolution of the phase shifters and the attenuators. This aspect is specifically taken into account to better understand the implementation in a real antenna array.

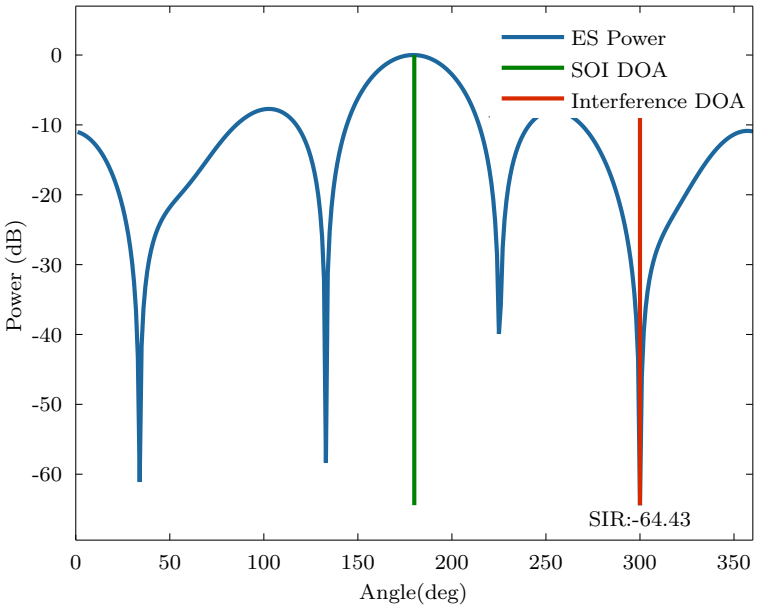


Figure 4.1: Beam pattern for the optimal null steering algorithm

In this section, the performance of the algorithm in general is discussed. For simulation purposes, the user signal is located at 180 degrees while the interferer takes integer values in the range 1-360 degrees. The effect of the relative position of the interferer with respect to the user is analyzed in two different cases.

Case I: Null Inside the Main Beam: When the interference signal's DOA is located close to the user signal's DOA, the null steering algorithms, studied in Chapter 3, do not perform as expected. The null depth starts to degrade in value and the null pointing angle error increases as the interference signal is close in angle to the user signal, as presented in the following example, Figure 4.4.

Figure 4.4 shows the beam pattern of the optimal null steering algorithm when the interference signal is located at 200° and the user signal is located at 180°. The

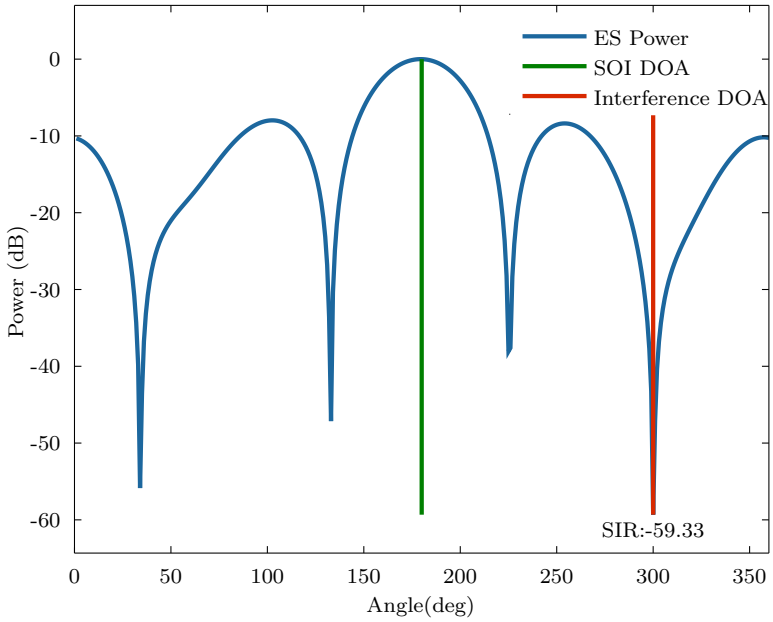


Figure 4.2: Beam pattern for the waveform modification null steering algorithm

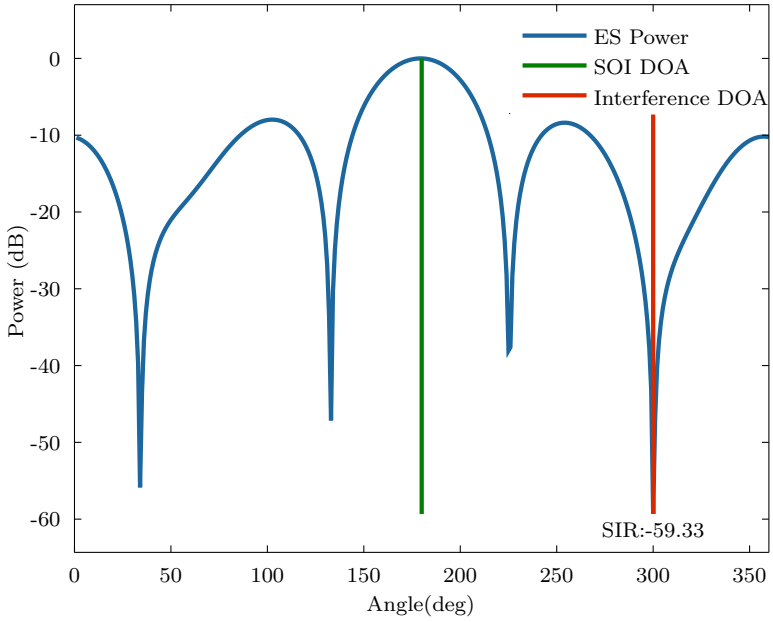


Figure 4.3: Beam pattern for the adaptive null steering algorithm

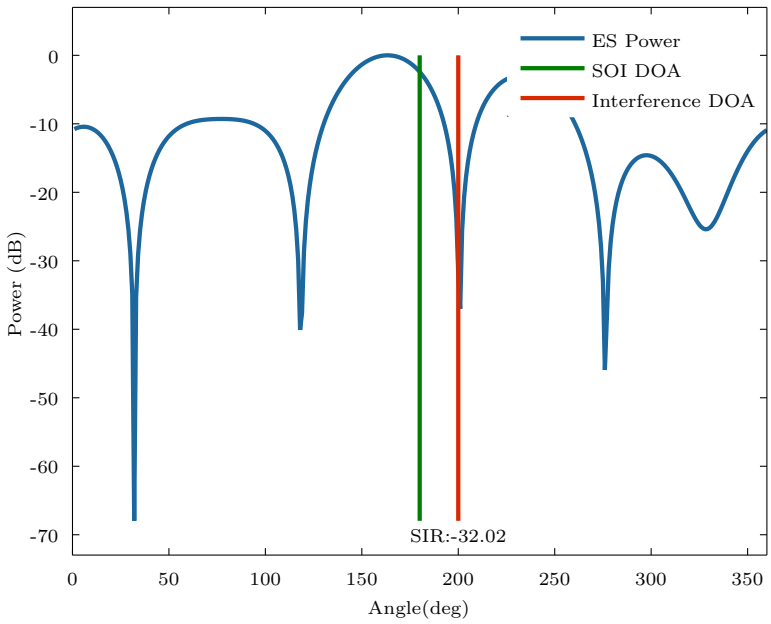


Figure 4.4: Beam pattern for case I

measured SIR in this case is 32 dB. Note that in this case the main beam is pointing towards 160°.

Monte Carlo simulations, with 1000 samples and 100 runs were performed to extract the statistics of the null steering algorithms in the case that the interference signal is located inside the main beam of the user's signal. The user's signal is fixed at 180° and the interference signal direction ranges from 130° to 230°, which represents the bound angle values for the main beam of the user's signal at 180°. From the statistics extracted, two parameters were of importance. Find the probability that SIR is higher than 40 dB and the performance of the algorithms, i.e. the value of the SIR, for a probability of 75 %.

Figure 4.5 shows the results of this simulation for the optimal null steering algorithm. The cumulative distribution function shows that the SIR will be higher than 40 dB with a probability of 33%; and 75% of the time the SIR will be higher

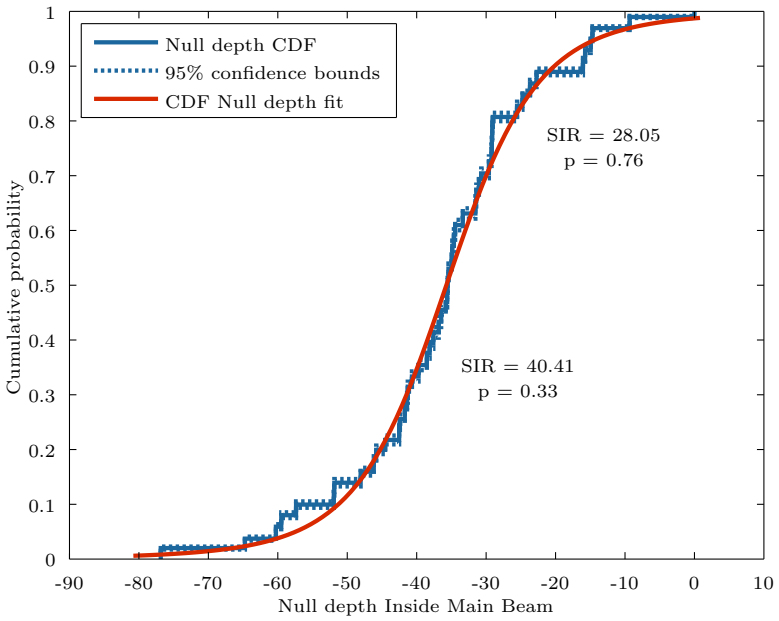


Figure 4.5: CDF for case I using the optimal null steering algorithm

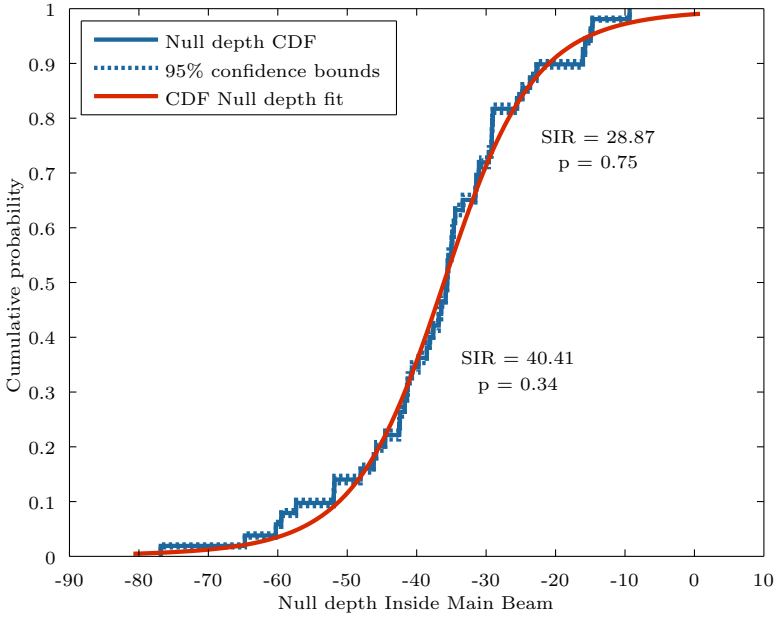


Figure 4.6: CDF for case I using the waveform modification algorithm

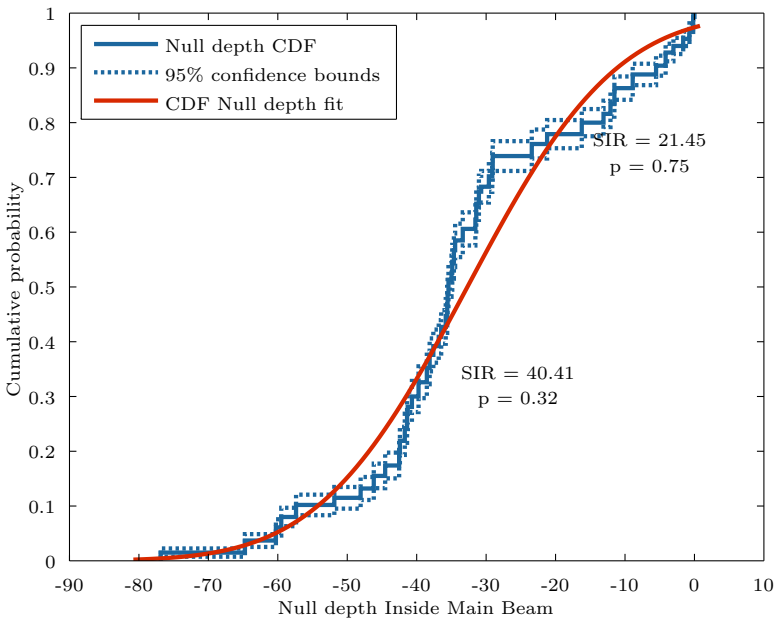


Figure 4.7: CDF for case I using the LMS algorithm

Table 4.3: CDF Values Summary for Case I

Method	SIR [dB] ($p \geq 0.75$)	p (SIR $\geq 30dB$)
Optimal null steering	28.05	0.65
Waveform modification	28.05	0.64
LMS null steering	21.45	0.63

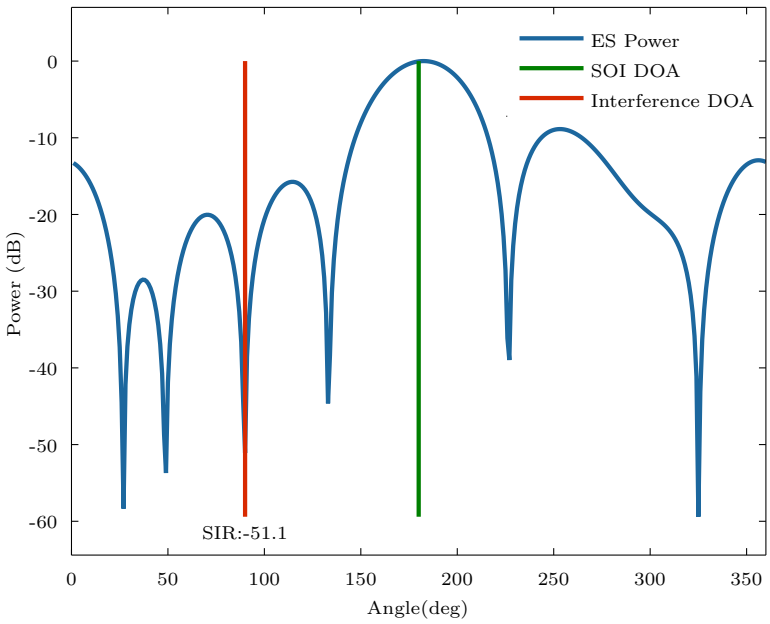


Figure 4.8: Beam pattern for case II

than 28 dB. Similar analysis was performed for the LMS null steering algorithm and the waveform modification algorithm. The resulting CDFs for these algorithms are presented in Figures 4.6 and 4.7. The results are summarized in Table 4.3.

Case II: Null Outside the Main Beam: In this section, the performance of the null steering algorithms is explored when the interference signal's DOA is located outside the main beam of the user's signal.

Figure 4.8 shows the results of the null steering algorithm when the interference signal is located at 90° and the user signal is located at 180°. The measured SIR in this case is 51 dB. Note that in this case the main beam is pointing towards 180° and there is no error in the null pointing angle.

Monte Carlo simulations described in the previous section were performed. The user's signal is fixed at 180° and the interference signal ranges from 1° to 130°, and

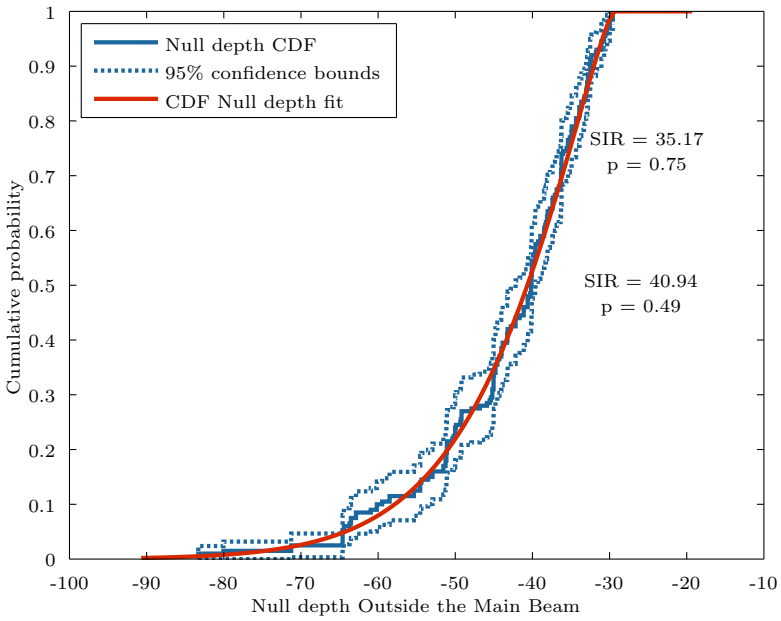


Figure 4.9: CDF for case II using the optimal null steering algorithm

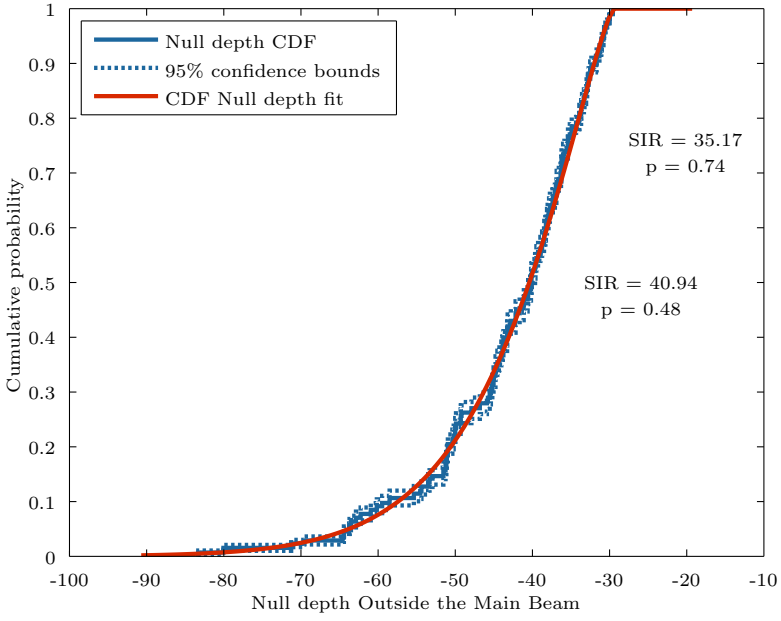


Figure 4.10: CDF for case II using the waveform modification algorithm

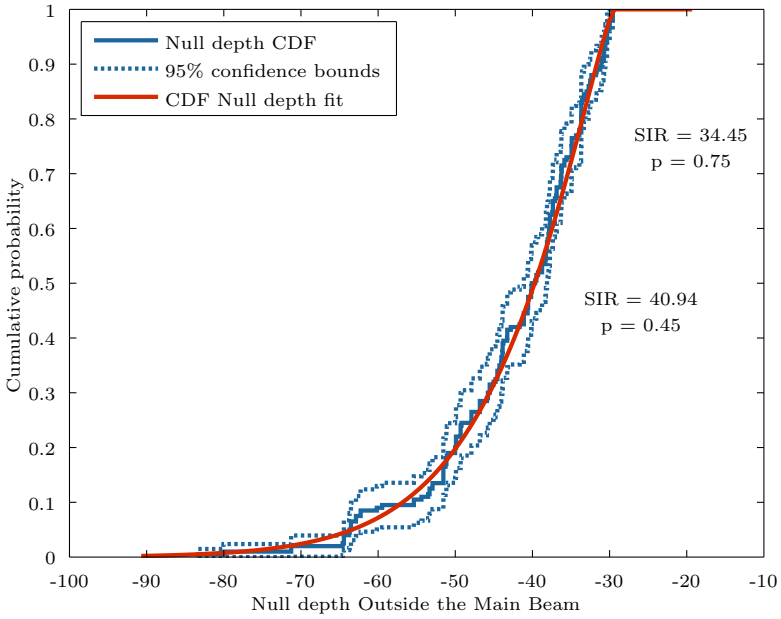


Figure 4.11: CDF for case II using LMS null steering algorithm

230° to 360°. From the statistics extracted, two parameters were of importance: the probability that SIR is higher than 40 dB and the performance of the algorithms, i.e. the value of the SIR, for a probability of 75 %.

Figure 4.9 shows the results of this simulation for the optimal null steering algorithm. The cumulative distribution function shows that the SIR will be higher than 40 dB with a probability of 33%; and 75% of the time the SIR will be higher than 28 dB. Similar analysis was performed for the LMS null steering algorithm and

Table 4.4: CDF Values Summary for Case II

Method	SIR [dB] ($p \geq 0.75$)	p (SIR $\geq 30dB$)
Optimal null steering	35.17	0.96
Waveform modification	35.75	0.98
LMS null steering	34.45	0.95

the waveform modification algorithm. The resulting CDFs for these algorithms are presented in Figures 4.10 and 4.11. The results are summarized in Table 4.4.

Phase and Magnitude Errors

Phase and magnitude errors on the null steering weights are not possible to avoid during hardware implementation. This section analyzes the effect of those errors in the performance of the null steering algorithms described in Chapter 3.

The quantization errors have an effect on the output of the algorithms: they affect null depth as well as the null direction. This effect has been studied through a Monte Carlo simulation for each algorithm as described below.

Phase Error Analysis

Consider the scenario where the user signal DOA is 180° and the interference signal DOA is 45°. In this scenario, phase errors on the weights are introduced to analyze the effect on the performance of the algorithms. Figure 4.12 shows the resulting beam pattern for different sets of phase-errors introduced into the phase of the null steering weights. The phase values of the null steering weights, after the introduction of the errors, oscillate ±10% their initial values. The error follows an arctangent distribution due to the nature of the phases of the weights of the antenna.

Note that the main beam pointing angle still points toward the direction of the signal user. However, the null pointing angle, as well as the null depth, is changed with the introduction of the phase errors.

A Monte Carlo simulation, with 1000 samples and 100 runs, was set up to study the performance of the null steering algorithms in terms of the null depth, the SIR, and the null pointing angle.

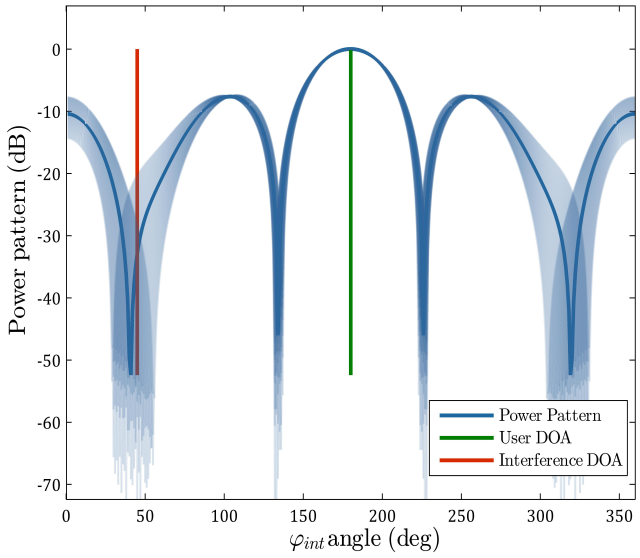


Figure 4.12: Effect of the phase errors on the power pattern

The results of the effect are presented in Figures 4.13, 4.14, and 4.15. These results shows the effects of errors in the phase in the performance of the null steering in terms of the SIR, defined in equation 3.5.

From these figures, it is possible to note interesting effects of the errors in the performance of the algorithms. The plots in Figures 4.13 - 4.15 show that the best performance of the algorithms, i.e. higher SIR, is obtained when the error tends to zero or is less than 4 %. When the phase error reaches values higher than 6 %, the SIR, on average, drops to 30 dB. Errors above 8 % have a negative effect on the SIR. For phase-errors higher than 8% the SIR drops below 20 dB.

However, it is interesting to note that at some specific angles, the errors have no effect in performance of the algorithms or even improve the performance of the algorithms. For example, in Figure 4.13, note that for the optimal null steering the effects of the errors at 150 ° have minimum incidence on the SIR. In this case the SIR

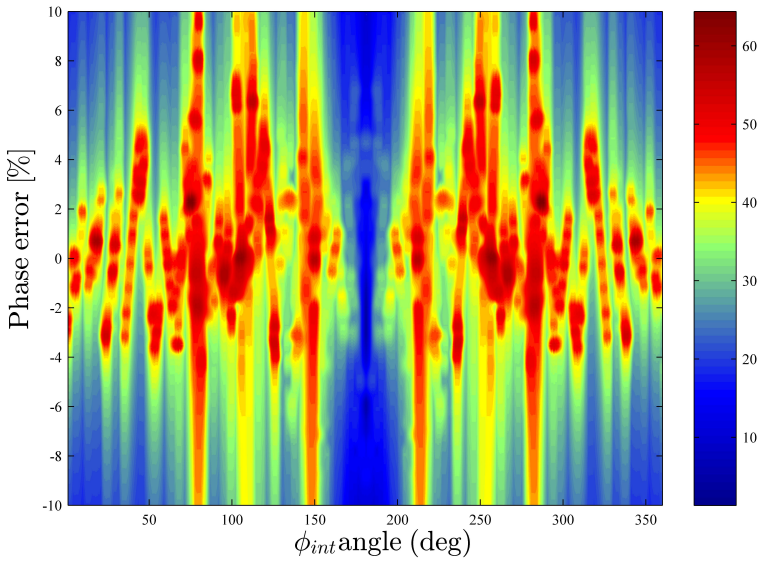


Figure 4.13: Effect of the phase error for the optimal null steering algorithm

remains constant between 40 dB and 60 dB, even with a 10 % error introduced to the phase.

Another interesting example is given at 300°. The null-depth with no error improves when the phases of the weights are introduced with an error of -4% as shown in Figure 4.14 for the waveform modification: the SIR improves from 40 dB up to 60 dB. This behavior is also present in the other two algorithms at different directions, shown in Figures 4.13 and 4.15.

The 3-dimensional (3D) power plots in function of the phase errors are shown in Figure 4.16, 4.17, 4.18.

Magnitude Analysis

Consider the scenario where the user signal DOA is 180° and the interference signal DOA is 45°. In this scenario, magnitude errors on the weights are introduced to see the effect on the performance of the algorithms. Figure 4.19 shows the resulting

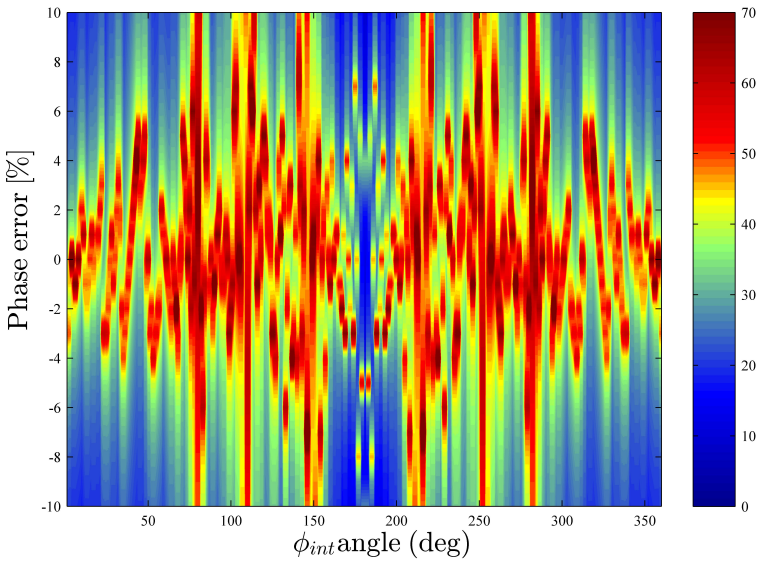


Figure 4.14: Effect of the phase error for the waveform modification algorithm

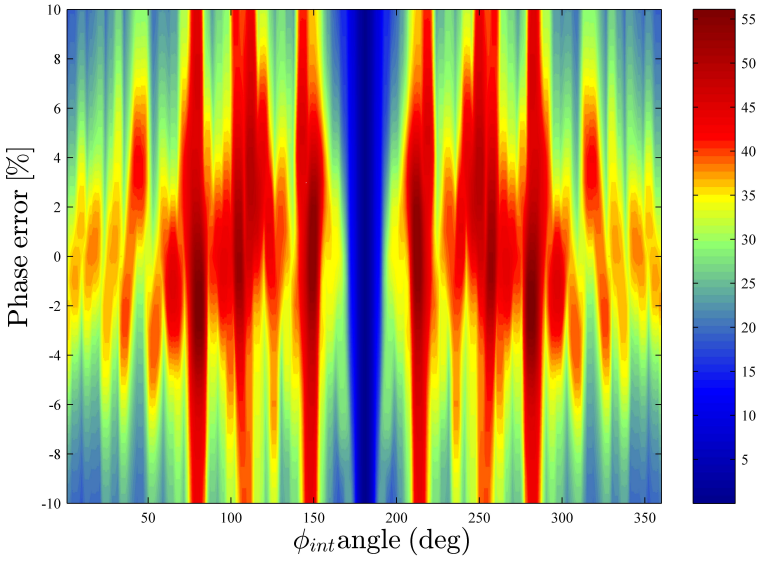


Figure 4.15: Effect of the phase error for the LMS null steering algorithm

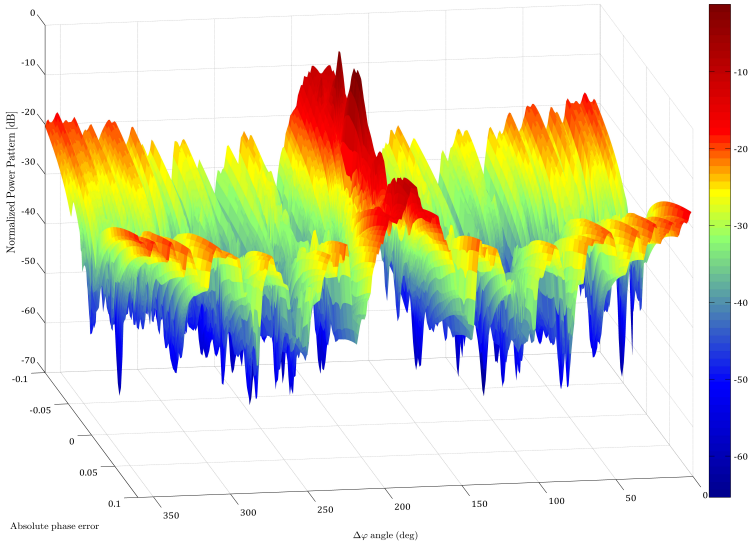


Figure 4.16: Effect of the magnitude error for the optimal null steering algorithm

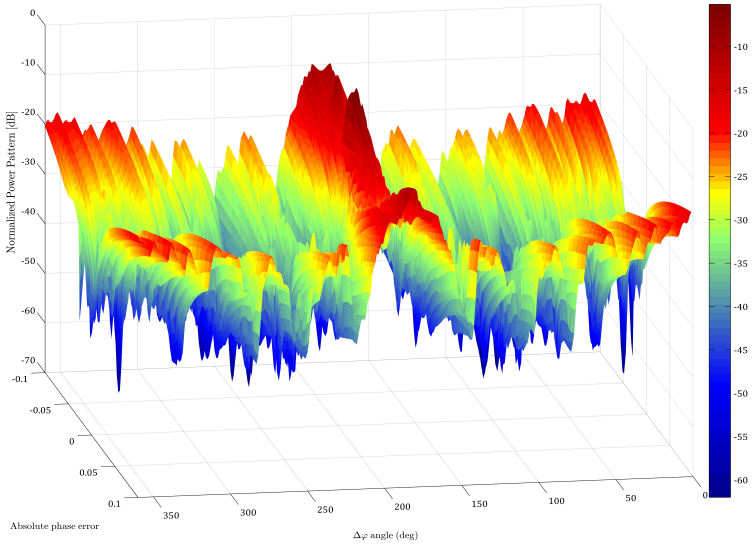


Figure 4.17: Effect of the magnitude error for the waveform modification algorithm

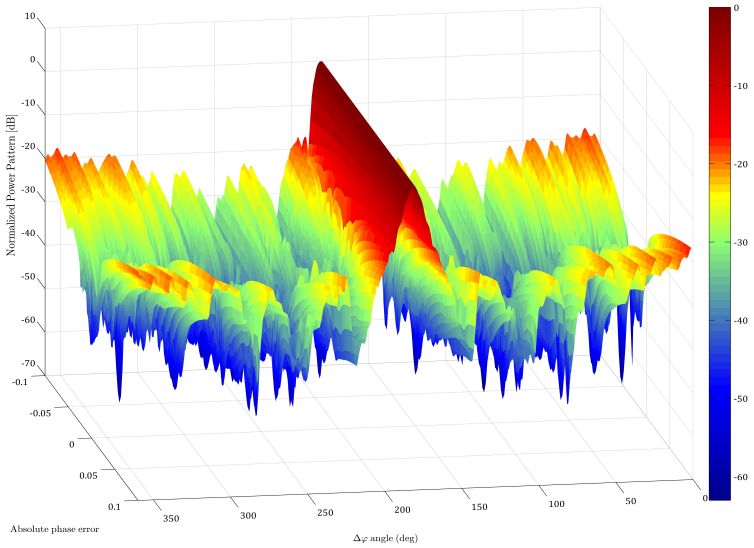


Figure 4.18: Effect of the magnitude error for the LMS null steering algorithm

power plot for different sets of magnitude-errors introduced into the magnitude of the null steering weights. Note that the main beam pointing angle still points toward the direction of the signal user. The null pointing angle, as well as the null depth, are changed with the introduction of the magnitude errors. However, as can be seen on Figure 4.19, the performance of the algorithms, with the addition of magnitude errors, is not as sensitive as in the case of phase errors. The magnitude values after the introduction of the errors oscillate $\pm 10\%$ their initial values. To better visualize the effect of the errors, the limits of the magnitude errors were increased up to 20%; even in this case the effect is minimum, as seen in Figure 4.20.

A Monte Carlo simulation was set up to study the performance of the null steering algorithms in terms of the null depth, the SIR, and the null pointing angle.

A magnitude error was introduced to the null steering weights. The error followed a Gaussian distribution due to the nature of the magnitude of the weights. The

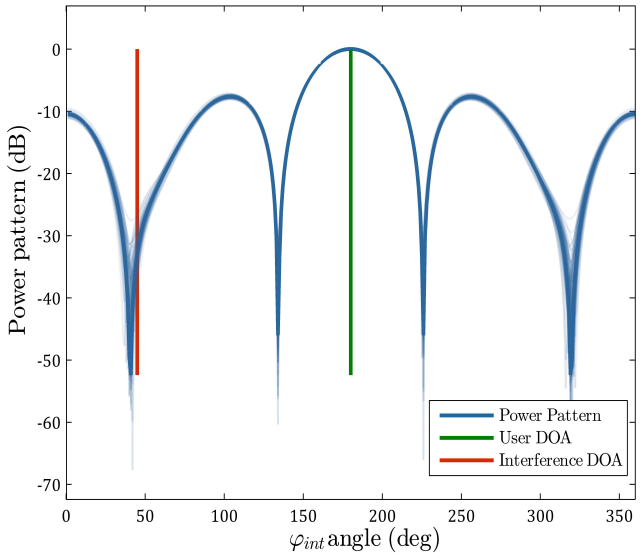


Figure 4.19: Effect of 10% magnitude error on the power pattern

results of the effect, in the performance of the null steering in terms of the SIR, as defined in equation 3.5, are presented in Figures 4.21, 4.22 and 4.23.

From these figures, it is possible to note the effect of the magnitude errors compared to the phase errors in the SIR, shown in Figures 4.21, 4.22 and 4.23. Note that the null depth remains almost constant for error changes in the magnitude of the weights.

Quantization Error and Phase Perturbation

In the previous sections, the uncertainties and quantization errors of the phase shifters and attenuators were taken into account for simulation purposes. The final goal of taking this approach is to best simulate the conditions in the real implementation.

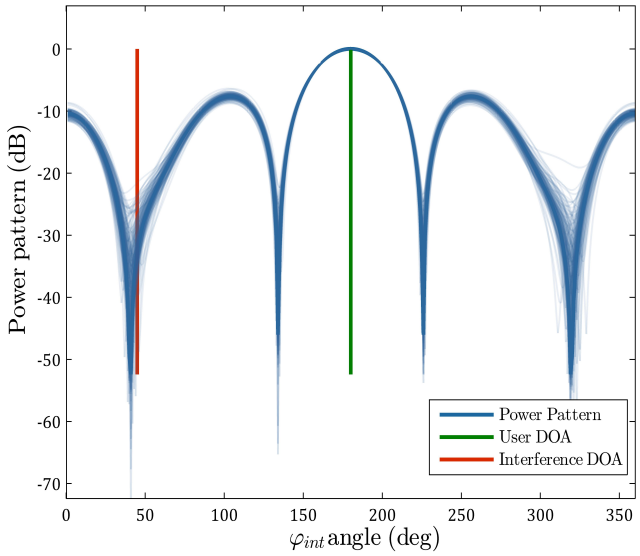


Figure 4.20: Effect of 20% magnitude error on the power pattern

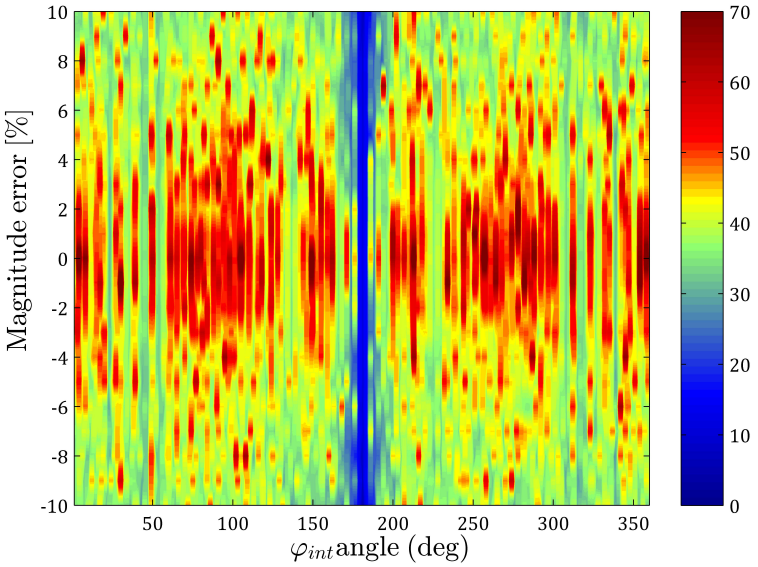


Figure 4.21: Effect of the magnitude error for the optimal null steering algorithm

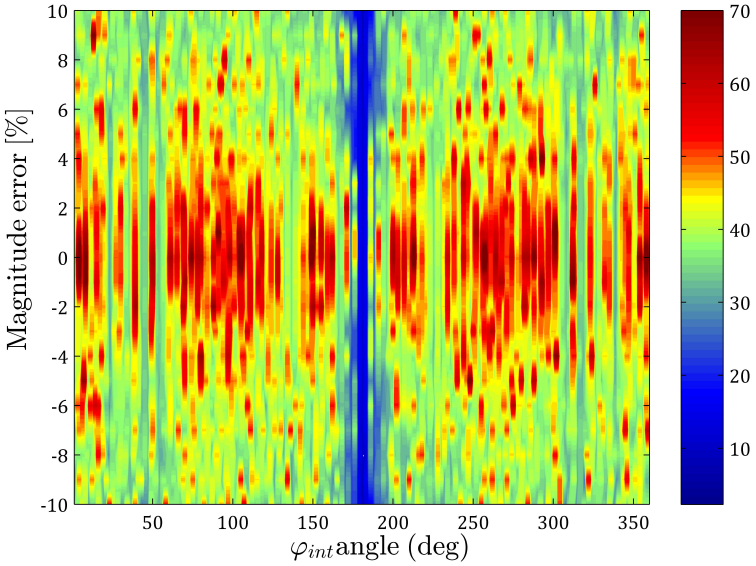


Figure 4.22: Effect of the magnitude error for the waveform modification algorithm

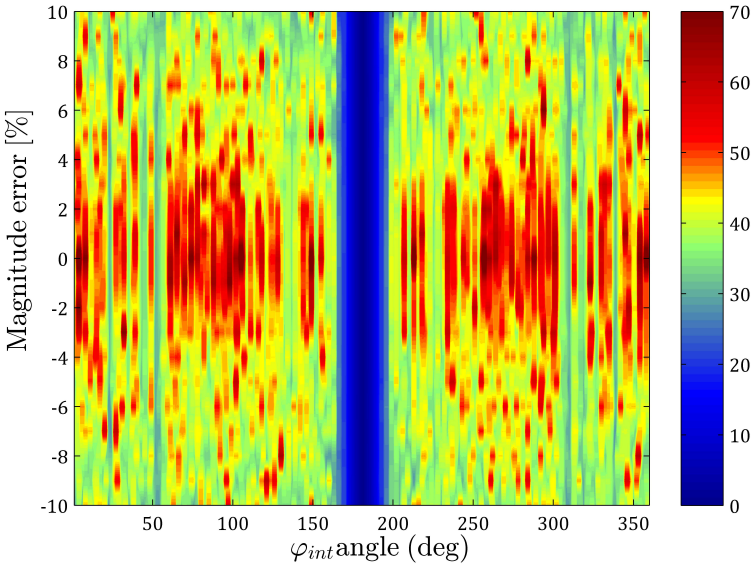


Figure 4.23: Effect of the magnitude error for the LMS null steering algorithm

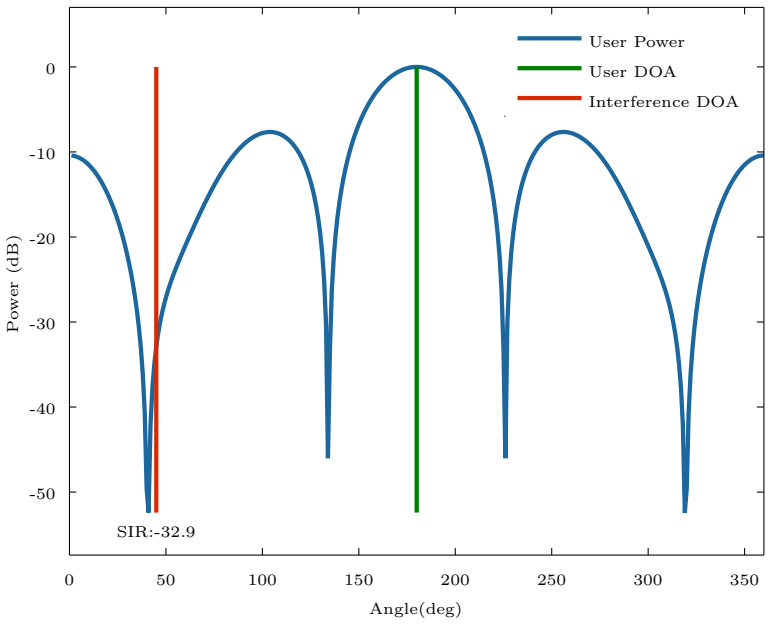


Figure 4.24: Beam pattern without phase perturbation

The quantized settings of the phase shifters and attenuators, i.e. the weights of the antenna array, limits the accuracy of the SIR and the null pointing angle. The next example illustrates this issue.

Figure 4.24 shows the null steering results using the optimal null steering algorithm presented in Chapter 3. The user signal is arriving from 180° and the interference signal is arriving from 45°. Note that the null pointing angle is shifted and it does not accurately point toward the interference signal. The obtained SIR in this case is 32 dB.

Figure 4.12 shows the behavior of the beam pattern when phase errors are present on the null steering weights. There are two main aspects worth noting. First, the main beam that is pointing in the direction of the user does not change and remains constant even though phase errors are introduced. Second, the null pointing angle,

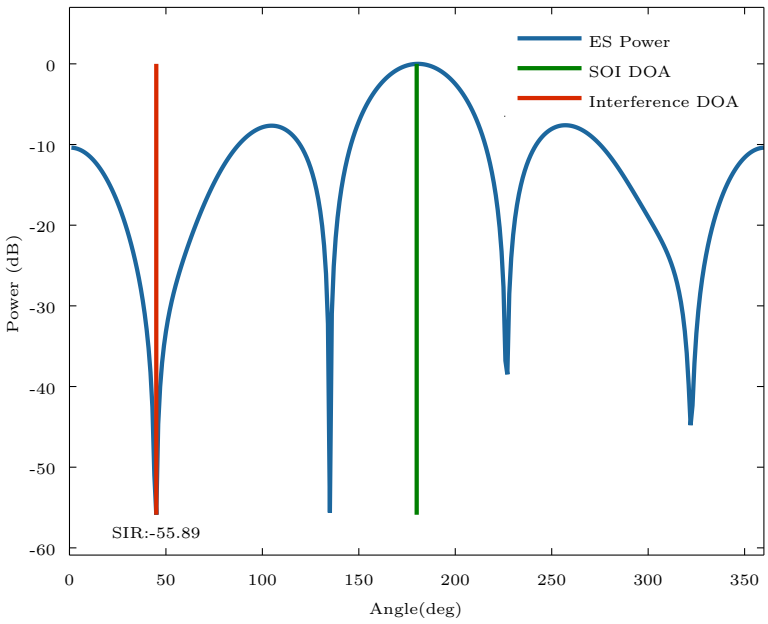


Figure 4.25: Beam pattern with phase perturbation

as opposed to the main beam pointing angle, moves along the interference direction for the same phase error. Therefore, it is possible to correct the null pointing angle, i.e. the SIR, by introducing controlled phase perturbations into the calculated null steering weights. The phase perturbations must follow the characteristics of the quantized steps of the phase shifters for practical purposes. This means that the phase perturbations must be discrete, i.e. in steps of 5.6°. The simulation results for the previous scenario, after adding the phase perturbation, are shown in Figure 4.25. The main beam points toward the desired direction: 180° in each simulation and does not change. However, the null pointing direction changes and improves the performance of the null steering system. The SIR obtained after the measurements is 55 dB. This represents an improvement of 23 dB on the SIR, reaching a *true optimum* in the null steering algorithms.

Table 4.5: Multi-null Steering Results for the Optimal Null Steering Algorithm

	φ_{int} [°]	SIR [dB]	Null angle [°]	Null depth [dB]	Pointing angle [°]
Null #1	30	-73.7	30	-73.7	138
Null #2	210	-36.2	213	-51.1	138
Null #3	280	-31.6	289	-38.6	138
Null #4	320	-39.2	318	-63.0	138

It is possible to perform equal analysis on the magnitude of the antenna array weights. However, as can be seen in Figures 4.21, 4.22, and 4.23, the effect of the magnitude errors in the weights sent to the beamformer is not considerable, as discussed in previous sections.

Multiple Nulls

Assume that the user is located at 135 ° and the interference signals are arriving at 30°, 210°, 280° and 320°. Figure 4.26 shows the beam pattern of the simulation results for multi-null steering using the optimal null steering algorithm. Table 4.5 shows the summary of the results obtained using this algorithm. The nulls are widely separated and the simulation result verifies the theory predicted by the algorithms.

The results show that there are nulls located at the interference angles summarized in Table 4.5.

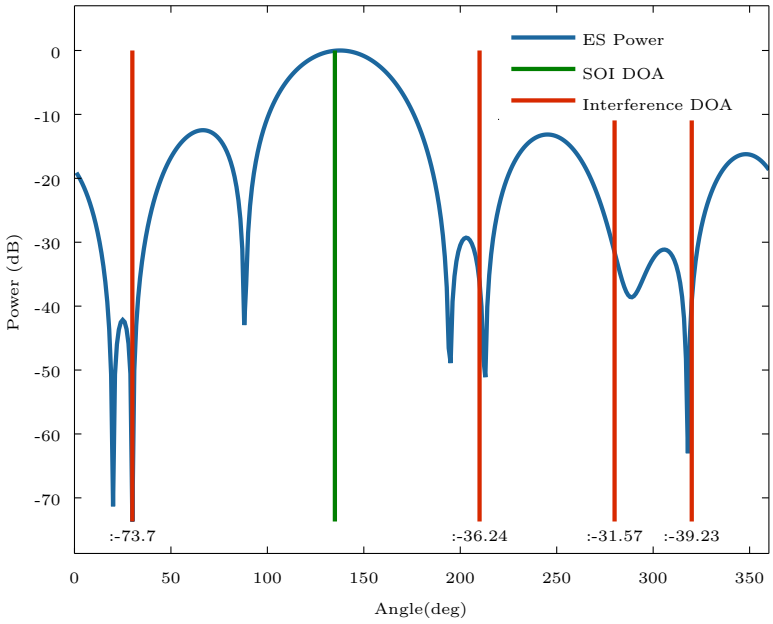


Figure 4.26: Beam pattern for the optimal multi-null steering algorithm

LAB TESTS

Experiments presented in this chapter are proof of concept. This chapter summarizes the experiment performed. Numerous tests have been performed to validate the simulations presented in Chapter 4.

The hardware implementation of the null steering system was achieved using the communications lab at Montana State University. This includes:

- implementation of algorithms, including hardware and software platforms;
- the test environment.

The hardware interface with the analog array and the lab test diagram is shown in Figure 5.1.

Lab Setup

The experiments were conducted in an anechoic chamber. The user and the interference signal were generated by continuous wave (CW) signal sources with a Signal to Noise Ratio (SNR) higher than 30 dB. The transmitter antenna was a horn antenna capable of transmitting RF signals from 4.9 to 7.05 GHz.

The receiver consisted of an 8-element circular antenna array. The attenuation and the phase shift for the elements were controlled by a beamformer that is part of the smart antenna system [25].

In order to capture the power pattern of the receiving antenna at different angles, the circular antenna array was placed on turntable equipped with a high resolution 0.1 degrees, stepper motor.

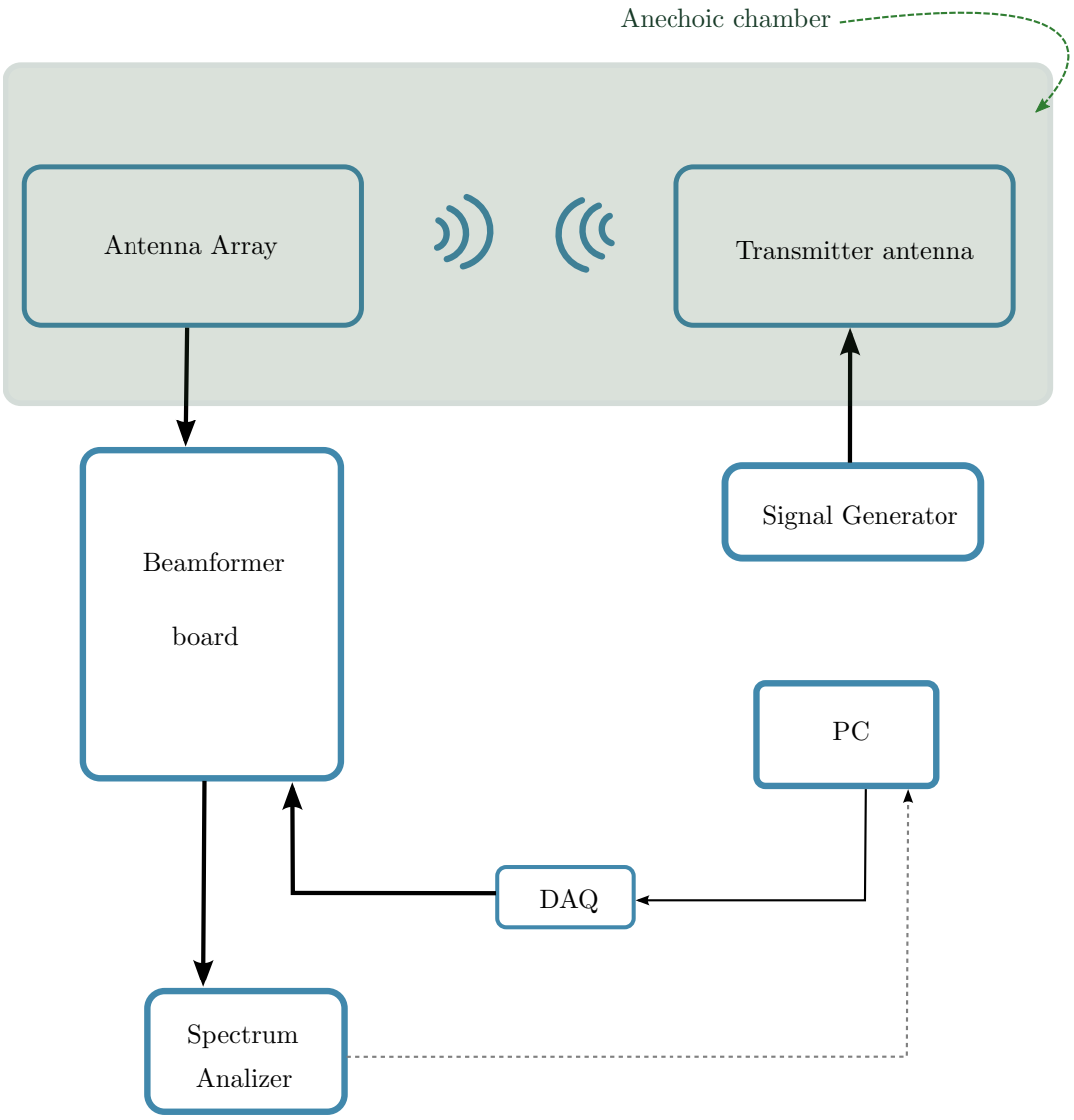


Figure 5.1: Block diagram of the lab test set up for receiving null steering

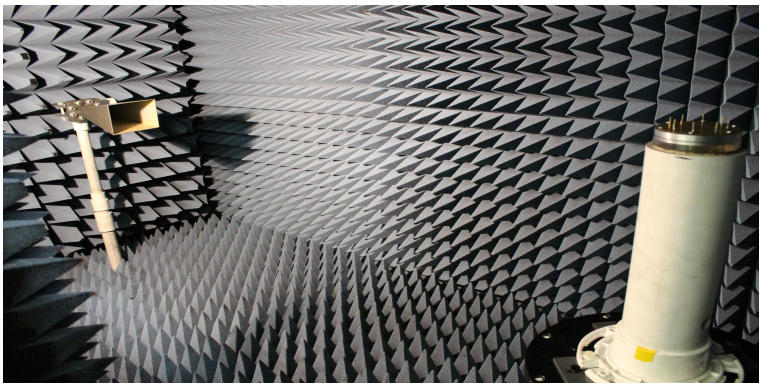


Figure 5.2: Anechoic chamber

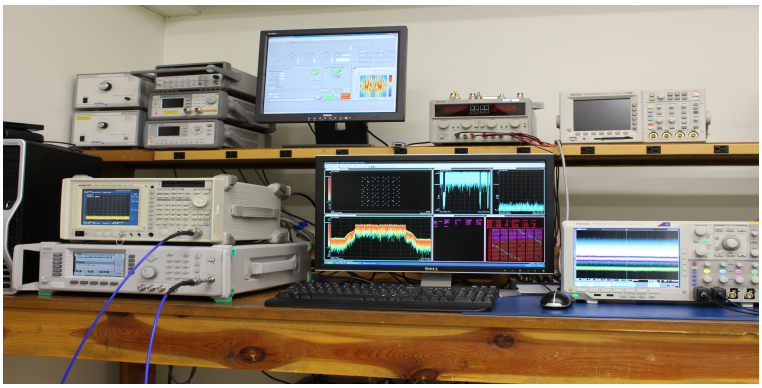


Figure 5.3: Instruments

Various MATLAB and LabVIEW scripts were used to control the hardware in the anechoic chamber.

A 68369 A/NV Anritsu signal generator used to send a CW signal at 5.8 GHz to the transmitter. A R3273 Advantest Spectrum Analyzer was placed to measure the power received by the circular antenna array. A National Instruments DAQ card (PCI 6013) was used to provide an interface between the computer and the beamformer. Using this card and a LabVIEW script, it was possible to send the weights to the antenna to perform null steering and beamforming.

The system setup is shown in Figure 5.3 and refanant Initial work on the implementation is described in Weber [30], Panique [6], Tidd [25].

In order to obtain the power pattern for the null steering system, the weights are first calculated and then sent to the beamformer board. The null steering weights are calculated using the null steering algorithms described in Chapter 2. The beamformer board is an eight channel system, each channel equipped with a 6−bit phase shifter and a 6−bit attenuator. Therefore, the complex weights have to be transformed into 6−bit form, before being sent to the beamformer board. A custom MATLAB script was designed to perform this transformation. After the null steering weights are sent to the beamformer board, the antenna array is placed inside the anechoic chamber with all necessary connections. Then, the Anritsu signal generator sends an RF CW signal at 5.8 GHz to the transmitter antenna.

The signal coming from the horn antenna is then received by the UCA; processed by the eight channel beamformer board; and after processing, the signal is sent to the spectrum analyzer to measure the energy from the signal received. The null steering weights are calculated using the null steering algorithms described in Chapter 2. At this point, the assumption is that the antenna main lobe is located at 0° with respect to the main user signal. To measure the power spectrum with a resolution of 1 degree, the circular antenna array is rotated and the energy of the signal is measured. The rotation process is automated by the turntable, which is controlled by a personal computer. The signal arriving at the antenna array is measured at every angle of arrival, i.e. from 1 to 360 degrees. A MATLAB script was written for post-processing purposes. After the measurements were finished, it was possible to obtain the SIR as well as the pointing angle to verify the performance of the Null Steering system.

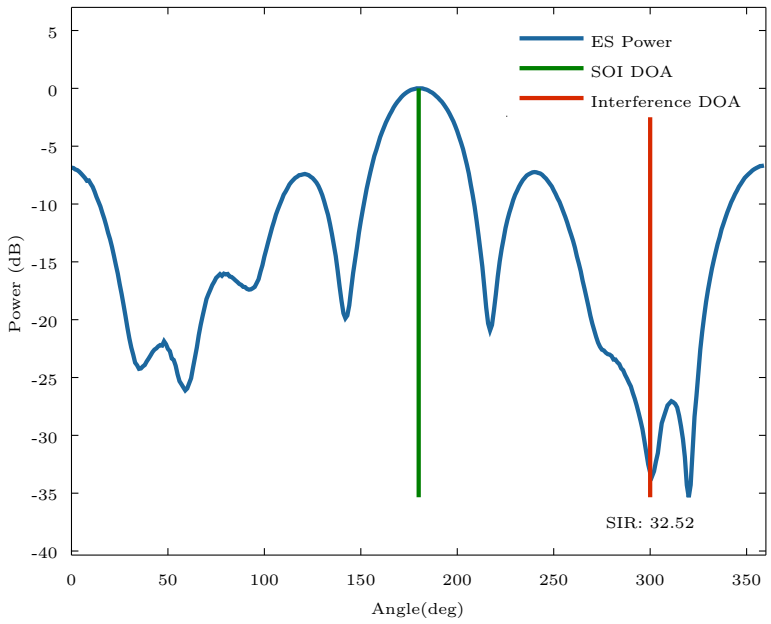


Figure 5.4: Beam pattern for the optimal null steering algorithm

Lab Test Results

The three algorithms described in Chapter 3 were implemented on a personal computer that calculates the weights. For the first algorithm, the perturbed patterns of imposing one null at 300 degrees is shown in Figure 5.4.

Note that for the optimal null steering algorithm, the obtained SIR reaches up to 32 dB. The null pointing angle for this measurement does not present error. There, the null imposed at the interference DOA (300°) can be clearly observed.

Similar measurements were performed for the waveform modification null steering algorithm. The results is presented in Figure 5.5. The weights sent to the beamformer are summarized in Table 5.1. In this case, the SIR obtained using this method is 36 dB. There is no error in the null pointing angle in this case.

Table 5.1: Experimental Null Steering Results

Method	φ_d [°]	φ_{int} [°]	SIR[dB]
Optimal null steering	180	300	32.52
Waveform modification	180	300	36.00
LMS null steering	180	300	34.18

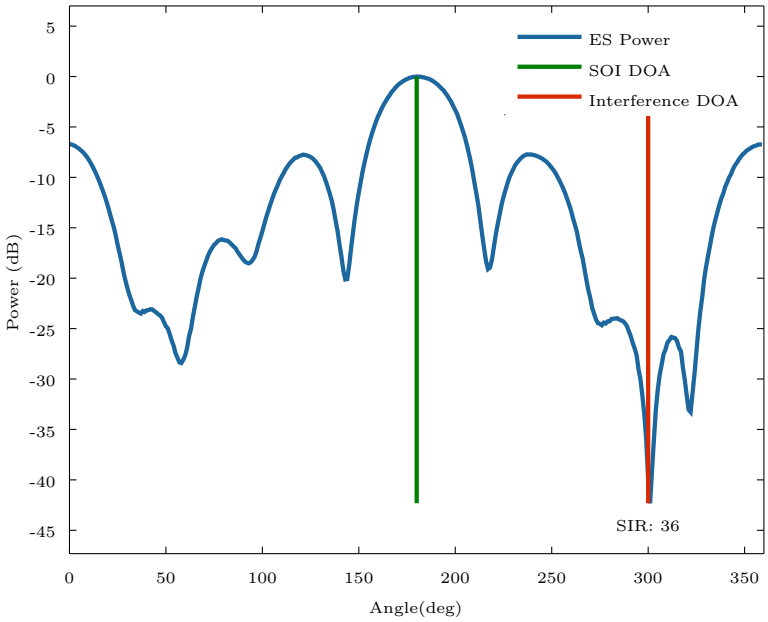


Figure 5.5: Beam pattern for the waveform modification null steering algorithm

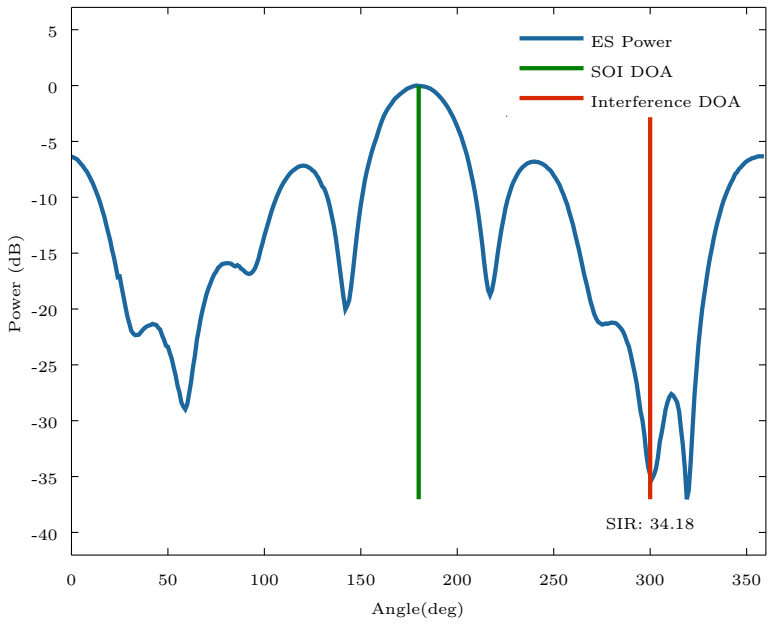


Figure 5.6: Beam pattern for the LMS adaptive null steering algorithm

Finally, the results for the measurements using the LMS adaptive null steering algorithm is presented in Figure 5.6. Note that, in this case, the SIR obtained is 34 dB.

All the measured results presented have reached SIR values higher than 30 dB for the described setup.

CONCLUSION AND FUTURE WORK

Conclusions

Null steering algorithms for a compact analog array were successfully implemented.

- A simulation study was carried out to validate the performance of the null steering algorithms, and all achieve deep nulls at the interference angular location.
- Three algorithms were implemented. Two of the algorithms calculated the weights analytically allowing a fast null steering operation with prior knowledge of the direction of arrival of the signals. The third algorithm calculated the null steering weights adaptively, allowing a simple implementation without prior estimation of the direction of arrival.
- Realistic considerations were taken into account to accurately model the null steering algorithms when implemented in hardware.
- The effect of the phase and amplitude oscillations of the null steering weights on the performance of the algorithms was analyzed.
- The effect of the weight quantization error on the null placement was analyzed. The quantization errors in the phase were proven to have more impact than quantization errors in amplitude on the performance of the null steering algorithms.
- By introducing discrete phase perturbations, the performance of the null steering algorithms was improved in terms of the SIR. The performance improvement on the SIR was up to 20 dB.

- Real implementation of the null steering algorithms was performed using an 8 element uniform circular array.
- By measuring the power pattern of the antenna array, the SIR was obtained. A SIR up to 36 dB was measured in a real scenario.
- The measured results proved the validity of the null steering algorithms. In spite of the unpredictable fluctuation on the actual implementation, the analog array performs extremely well for interference cancellation, considering the SIR obtained.

Future Work

The algorithms analyzed have been optimized from a general perspective without considering a particular application. Additional work is needed to implement null steering algorithms, taking into account application specific properties of real scenarios.

In this thesis, the null steering algorithms considered changes in the amplitude and phase mainly due to the hardware availability. Phase-only null steering algorithms should be implemented to simplify the hardware implementation.

REFERENCES CITED

[1] Emanuele Lopelli, Johan v. d. Tang, Arthur H. M. van Roermund, and SpringerLink (Online service). *Architectures and synthesizers for ultra-low power fast frequency-hopping WSN radios*. Springer Netherlands, Dordrecht, 2011. ISBN 9400701837, 9789400701823, 9400701829, 9789400701830.

[2] Bluetooth standard description. `http://www.bluetooth.com`. Accessed: 2014-03-30.

[3] Yingying Chen, Wenyuan Xu, Wade Trappe, and Yanyong Zhang. *Jamming Attacks and Radio Interference*, pages 1–13. Springer US, Boston, MA, 2009. ISBN 9780387884905, 0387884904.

[4] A. Mpitziopoulos, A. Mpitziopoulos, D. Gavalas, D. Gavalas, C. Konstantopoulos, C. Konstantopoulos, G. Pantziou, and G. Pantziou. A survey on jamming attacks and countermeasures in wsns. *IEEE Communications Surveys & Tutorials*, 11(4):42–56, 2009.

[5] H. Condori-Quispe, R.J. Weber, and Yikun Huang. Nullsteering with an analog array. In *Aerospace Conference*, March 2014.

[6] Michael D. Panique. Design and evaluation of test bed software for a smart antenna system supporting wireless communication in rural area, 2008. Master thesis, Montana State University.

[7] M. Mouhamadou and P. Vaudon. Technique based on sqp algorithm for antenna array pattern synthesis: Beam and null steering. In *Electromagnetic Field Computation, 2006 12th Biennial IEEE Conference on*, pages 383–383, 2006. doi: 10.1109/CEFC-06.2006.1633173.

[8] Hu Zhu, Lizhen Deng, and Xiaodong Bai. Phase-only direct data domain adaptive processing algorithm using hybrid genetic algorithms. In *Communication Technology (ICCT), 2012 IEEE 14th International Conference on*, pages 951–955, Nov 2012. doi: 10.1109/ICCT.2012.6511335.

[9] F. Ananasso. Nulling performance of null-steering arrays with digital phase-only weights. *Electronics Letters*, 17(7):255, 1981.

[10] Randy L. Haupt and S.E. Haupt. Phase-only adaptive nulling with a genetic algorithm. In *Aerospace Conference, 1997. Proceedings., IEEE*, volume 3, pages 151–160 vol.3, Feb 1997. doi: 10.1109/AERO.1997.574858.

[11] T. Vu. Null steering by controlling current amplitudes only. In *Antennas and Propagation Society International Symposium, 1984*, volume 22, pages 811–814, June 1984. doi: 10.1109/APS.1984.1149137.

[12] N.T. Yallaparagada, G.R. Hardel, D. Mandal, and A.K. Bhattacharjee. Genetic algorithm for null synthesizing of circular array antennas by amplitude control. In *Computers Informatics (ISCI), 2011 IEEE Symposium on*, pages 1–5, March 2011. doi: 10.1109/ISCI.2011.5958873.

[13] Benjamin Friedlander and B. Porat. Performance analysis of a null-steering algorithm based on direction-of-arrival estimation. *Acoustics, Speech and Signal Processing, IEEE Transactions on*, 37(4):461–466, April 1989. ISSN 0096-3518. doi: 10.1109/29.17526.

[14] Yikun Huang and M. Panique. Performance analysis of a null steering algorithm. In *Antennas and Propagation Society International Symposium, 2007 IEEE*, pages 4212–4215, June 2007. doi: 10.1109/APS.2007.4396470.

[15] R.A. Qamar and N.M. Khan. Null steering, a comparative analysis. In *Multitopic Conference, 2009. INMIC 2009. IEEE 13th International*, pages 1–5, Dec 2009. doi: 10.1109/INMIC.2009.5383130.

[16] H.M. Elkamchouchi and M.A.R.M. Adam. A new constrained fast null steering algorithm. In *Antennas and Propagation Society International Symposium, 2000. IEEE*, volume 2, pages 926–929 vol.2, July 2000. doi: 10.1109/APS.2000.875371.

[17] W. Tidd, Yufei Zhao, and Yikun Huang. A compact beamspace doa estimation and beamforming communication device. In *Aerospace Conference, 2011 IEEE*, pages 1–8, March 2011. doi: 10.1109/AERO.2011.5747311.

[18] W. Tidd, Yikun Huang, and Yufei Zhao. Sequentical beamspace beamforming. In *Aerospace Conference, 2012 IEEE*, pages 1–8, March 2012. doi: 10.1109/AERO.2012.6187088.

[19] R.J. Weber and Yikun Huang. A cognitive beamforming array. In *Phased Array Systems and Technology (ARRAY), 2010 IEEE International Symposium on*, pages 348–356, Oct 2010. doi: 10.1109/ARRAY.2010.5613346.

[20] R.J. Weber and Yikun Huang. An automatic calibration system for smart antenna arrays. In *Antennas and Propagation Society International Symposium, 2009. APSURSI '09. IEEE*, pages 1–4, June 2009. doi: 10.1109/APS.2009.5171470.

[21] W. Tidd and Yikun Huang. An experimental evaluation of a novel sequential beamspace smart antenna system. In *MILITARY COMMUNICATIONS*

CONFERENCE, 2011 - MILCOM 2011, pages 583–588, Nov 2011. doi: 10.1109/MILCOM.2011.6127736.

[22] A. Khallaayoun, A. Olson, M.D. Panique, and Yikun Huang. An adaptive smart antenna testbed for wimax radio. In *Mobile WiMAX Symposium, 2009. MWS '09. IEEE*, pages 209–213, July 2009. doi: 10.1109/MWS.2009.36.

[23] R.J. Weber and Yikun Huang. A frequency agile beamforming array. In *Antennas and Propagation (APSURSI), 2011 IE11EE International Symposium on*, pages 2035–2038, July 2011. doi: 10.1109/APS.2011.5996907.

[24] Yikun Huang. Wimax dynamnic beamforming antenna. *Aerospace and Electronic Systems Magazine, IEEE*, 23(8):26–31, Aug 2008. ISSN 0885-8985. doi: 10.1109/MAES.2008.4607896.

[25] William G. Tidd. Sequential beamspace smart antenna system, 2011. Master thesis, Montana State University.

[26] Yikun Huang, W. Tidd, A. Olson, and R.S. Wolff. A compact smart antenna for wimax radio. In *Mobile WiMAX Symposium, 2009. MWS '09. IEEE*, pages 169–173, July 2009. doi: 10.1109/MWS.2009.37.

[27] W. Tidd, Yufei Zhao, and Yikun Huang. Sequential beamspace doa estimation. In *Antennas and Propagation (APSURSI), 2011 IEEE International Symposium on*, pages 2817–2820, July 2011. doi: 10.1109/APS.2011.5997112.

[28] Yikun Huang. Design of a dynamic beamforming antenna for wimax radio systems. In *Aerospace Conference, 2008 IEEE*, pages 1–6, March 2008. doi: 10.1109/AERO.2008.4526317.

[29] R.J. Weber, Yikun Huang, and W. Tidd. Cognitive beamforming antenna. In *Aerospace Conference, 2010 IEEE*, pages 1–8, March 2010. doi: 10.1109/AERO.2010.5446968.

[30] Raymond J. Weber. Development of a cognitive array system, 2010. Master thesis, Montana State University.

[31] Constantine A. Balanis and Knovel (Firm). *Antenna theory: analysis and design*. Wiley, Hoboken, N.J, 2005. ISBN 1601193734, 9780471667827, 047166782X, 9781601193735.

[32] Bruce A. Black. *Introduction to wireless systems*. Prentice Hall, Upper Saddle River, N.J, 2008. ISBN 0132447894, 9780132447898.

[33] Yikun Huang and M. Panique. Performance analysis of a null steering algorithm. In *Antennas and Propagation Society International Symposium, 2007 IEEE*, pages 4212–4215, June 2007. doi: 10.1109/APS.2007.4396470.

[34] Constantine A. Balanis and Panayiotis I. Ioannides. *Introduction to Smart Antennas*, volume 5. Morgan & Claypool Publishers, San Rafael, 2007. ISBN 1598291769, 9781598291766, 1598291777, 9781598291773.